EXPERIMENTAL INVESTIGATION AND OPTIMIZATION OF LASER SURFACE TREATMENT PARAMETERS FOR 1.2379 (AISI D2) TOOL STEEL

A Thesis Submitted to
the Graduate School of Engineering and Sciences of
İzmir Institute of Technology
in Partial Fulfilment of the Requirements for the Degree of

MASTER OF SCIENCE

in Mechanical Engineering

by
Sayit ÖZBEY

June 2023
İZMİR

ACKNOWLEDGMENTS

I would like to thank my thesis advisor, Prof. Dr. Hatice Seçil ARTEM for her dedicated support, guidance and encouraging approach through the learning and writing process of my master thesis.

I would like to express my endless respect and thank my thesis co-advisor, Prof. Dr. Ersin KAYAHAN, who shared his knowledge and experience with me regarding the experimental part of my thesis.

I would like to thank the Laser Technology Research and Application Center (LATARUM) and its valuable employees for allowing me to use the devices and equipment which I used for my thesis experimental parts.

I sincerely thank Mrs. Hacer İrem ERTEN for her help and contributions to the regression and optimization part of my studies.

I would like to express my endless thanks to my precious family who have always supported me throughout my life.

We approve the thesis of **Sayit ÖZBEY**

Examining Committee Members:

Prof. Dr. H. Seçil ARTEM
Department of Mechanical Engineering, Izmir Institute of Technology

Assist. Prof. Dr. Kasım TOPRAK
Department of Mechanical Engineering, Izmir Institute of Technology

Assist. Prof. Dr. Suat Bahar BAŞTÜRK
Department of Mechanical Engineering, Manisa Celal Bayar University

22 June 2023

Prof. Dr. H. Seçil ARTEM
Supervisor, Department of Mechanical Engineering, Izmir Institute of Technology

Prof. Dr. Ersin KAYAHAN
Co-Supervisor, Department of Electro-Optical System Engineering, Kocaeli University

Prof. Dr. M. İ. Can DEDE
Head of the Department of Mechanical Engineering

Prof. Dr. Mehtap EANES
Head of the Graduate School of Engineering and Sciences

ABSTRACT

EXPERIMENTAL INVESTIGATION AND OPTIMIZATION OF LASER SURFACE TREATMENT PARAMETERS FOR 1.2379 (AISI D2) TOOL STEEL

Laser surface treatment has been used as a cost-effective method to improve the surface qualities of materials, such as hardness, strength, roughness, corrosion resistance, chemical resistance and coefficient of friction by modifying their structure and physical features using laser beam heat. In this thesis, surface properties such as hardness and roughness of 1.2379 cold work tool steel, a commonly used material in the die and mold industries for injection mold inserts, were investigated both experimental and numerical (regression analysis, optimization) studies. In the experimental part of the thesis, 1.2379 cold work tool steel surface was treated using a commercially available industrial Ytterbium low-power pulsed fiber laser. Laser parameters including average power, repetition rate, line spacing and scan speed were considered as input parameters while hardness and roughness were used as output parameters. Input parameters used in the experiments were produced by using a 3^4 full factorial design. The effect of laser parameters on the surface properties of 1.2379 cold work tool steel was investigated by hardness and roughness measurements. Using the results of the measurements different regression models were conducted and the best fit was chosen. As a result of regression analysis, it is obtained that the second-order multiple non-linear model is the best regression equation for hardness and the second-order logarithmic multiple non-linear model is the best for roughness

Following the experimental study and regression analysis, an optimization study was performed using Wolfram MATHEMATICA 11.3 to determine the optimum laser parameters for the hardness and roughness of 1.2379 cold work tool steel. In the optimization, Random Search (MRS), Simulated Annealing (MSA), Differential Evolution (MDE) and Nelder-Mead (MNM) methods were used for different optimization scenarios. By determining the optimum parameters, this thesis contributes to enhancing the surface properties, hardness and roughness, of 1.2379 cold work tool steel.

ÖZET

1.2379 (AISI D2) TAKIM ÇELİĞİNİN LAZERLE YÜZEY İŞLEME PARAMETRELERİNİN DENEYSEL OLARAK İNCELENMESİ VE OPTİMİZASYONU

Lazerle yüzey işleme, lazer ışını ısısı ile malzemelerin yapılarını ve fiziksel özelliklerini değiştirmekte olup yüzey özelliklerini (mukavemet, sertlik, pürüzlülük, sürtünme katsayısı, kimyasal direnç ve korozyon) geliştirmek için kullanılan uygun maliyetli bir teknolojidir. Bu tezde, kalıp endüstrisinde enjeksiyon kalıbı kesici uçlarında yaygın olarak kullanılan 1.2379 soğuk iş takım çeliğinin sertlik ve pürüzlülüğü gibi yüzey özellikleri hem deneysel hem de sayısal (regresyon analizi, optimizasyon) çalışmalarla incelenmiştir. Tezin deneysel bölümünde, 1.2379 soğuk iş takım çeliği yüzeyi, ticari olarak temin edilebilen bir endüstriyel Ytterbium düşük güçlü darbeli fiber lazer kullanılarak işlenmiştir. Giriş parametreleri olarak lazer parametreleri olan ortalama güç, tekrarlama oranı, çizgi aralığı ve tarama hızı; çıkış parametreleri olarak ise sertlik ve pürüzlülük kullanılmıştır. Deneylerde kullanılan giriş parametreleri 3^4 tam faktöriyel deney tasarımı kullanılarak üretilmiştir. Lazer parametrelerinin 1.2379 soğuk iş takım çeliğinin yüzey özelliklerine etkisi sertlik ve pürüzlülük ölçümleri ile araştırılmıştır. Ölçüm sonuçları kullanılarak farklı regresyon modelleri oluşturulmuş ve en uygun model seçilmiştir. Regresyon analizi sonucunda, ikinci mertebeden çoklu doğrusal olmayan modelin sertlik için en iyi regresyon denklemi, ikinci mertebeden çoklu doğrusal olmayan logaritmik modelin pürüzlülük için en iyi regresyon denklemi olduğu elde edilmiştir.

Deneysel çalışma ve regresyon analizinin ardından Wolfram MATHEMATICA 11.3 kullanılarak 1.2379 soğuk iş takım çeliğinin sertliği ve pürüzlülüğü için optimum lazer parametrelerinin belirlenmesi amacıyla optimizasyon çalışması yapılmıştır. Farklı optimizasyon senaryoları için Random Search (MRS), Simulated Annealing (MSA), Differential Evolution (MDE) ve Nelder-Mead (MNM) yöntemleri kullanılmıştır. Optimum parametreleri belirleyerek, bu tez 1.2379 soğuk iş takım çeliğinin yüzey özelliklerini sertliğini ve pürüzlülüğünü iyileştirmeye katkıda bulunmaktadır.

To My Family…

TABLE OF CONTENTS

LIST OF FIGURES

LIST OF TABLES

CHAPTER 1

INTRODUCTION

1.1. Literature Review

Surface qualities such as roughness, hardness, wear resistance and corrosion resistance are required for industrial applications. These alloys are highly expensive, thus there is an interest in decreasing the price of components that meet these specifications. In this regard, laser surface treatment (LST) has been employed as a cost-effective technology to enhance the surface properties of materials by modifying their structure and physical features using laser beam heat [1]. Laser surface treatment of materials is a useful technology since it allows to improve attributes including roughness, strength, hardness, corrosion, coefficient of friction and chemical resistance in a variety of materials. This enhancement is not only appropriate for applications with high wear rates and cutting loads, but it may also be utilized to protect or extend the component's functional life by repairing microcracks on surfaces. Furthermore, by producing a changed surface layer using laser surface treatment, aesthetics can be improved [2]. The most common advantages of laser surface treatment over the other methods are;

- enable to control distortion and thermal penetration.
- to be chemically clean
- enable to control thermal profile and therefore location and shape of heat affected zone (HAZ)
- less after machining
- possibility of remote processing
- suitable for automation [3].

Surface quality of substrate materials can be improved through laser surface treatment by modifying phase composition, topography, and microstructure. Laser radiation (in the nm range) is absorbed by conduction electrons when incident on a substrate material. When these excited electrons collide with lattice ions, they rapidly heat up. The heat from this thin layer is delivered to the main substrate. As a result, a layer of material with a thickness greater than the usual radiation absorption depth is rapidly

heated. When the laser irradiation is turned off, the substrate material cools as heat is transferred. The interaction of the laser with the substrate can be seen in Figure 1.1.

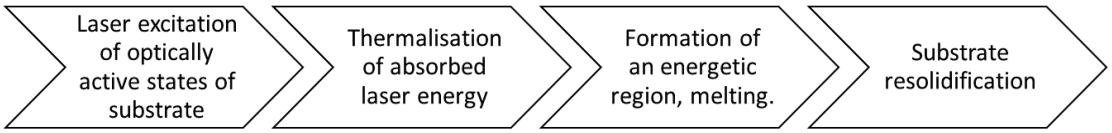

Figure 1.1. Laser material interaction

Since laser surface treatment process is extremely nonlinear, numerical modelling is required for a clear understanding of the process [4]. Vijay et. al. investigated an optimization study for surface roughness of stainless-steel parts during selective laser sintering process with the parameters of laser power, scan spacing and orientation. Taguchi method with L9 orthogonal array (OA) was preferred, and the optimal level of parameters was determined by the lower-the-better signal-to-noise (S/N) ratio. Moreover, analysis of variance (ANOVA) was applied to specify the most effected parameter and an empirical model was developed. Estimated optimum values in both approaches and experimental values were near enough (6.08 μm) [5].Matras et. al. studied optimization of surface roughness (Ra and Rz) by using laser scanning speed as a variable. A mathematical model was created and regression equations were developed by using ANOVA. The generated regression equations showed that the estimated and observed values are quite well matched. For parameter Ra, the R^2 determined as 0.87, while for parameter Rz is 0.78 [6].

Considering optimum experimental parameter for laser surface treatment is the main problem of industry. Laser parameter optimization can be performed with many methods. One of them is Taguchi method. Timur et al. used Taguchi method to consider optimum laser surface treatment parameters on Al 6082-T6 material. The effect of gas type pulse duration, pulse energy and focus position on laser surface treatment were investigated by using three levels. With this study it is obvious that which parameter have more effect on surface properties (roughness, porosity etc.)[7].

Surface hardness of laser treated AISI D2 tool steel was investigated with ANOVA and regression equations using a high power Nd:YAG fiber laser in Ref [8]. To assess the influence of the treated surface's heating temperature and feed rate on the surface hardness, hardening depths, width, angle and laser beam's energy density, linear and quadratic regression models were created. ANOVA revealed that both the linear and

quadratic regression model responses of the laser beam's energy density (Elb) and surface hardness (HRC) are significant (P-value<0.05). Results demonstrate that the main factor effect the hardness is the heating temperature and feed rate of the treated surface ,and determined as 1270 °C and 90 mm/min respectively.[8].

In Ref [9] the influence of the laser-polishing process employed on a milled and EDMed surface of 1.2379 tool steel was investigated. Two different industrial lasers, a 2.5 KW CO_2 laser and a high-power 3.1 KW diode laser (HPDL) were used to determine and optimize the laser parameters (power, feed and focal offset), resulting in a roughness reduction of up to 90% and mean roughness values (Ra) below 0.5 mm. Because of its martensitic structure, this steel is very challenging to polish. On the other hand, it also has a serious limitation due to the appearance of cracks with high thermal gradients. Due to the nature of laser polishing, which involves melting and subsequently solidifying metals with high thermal gradients in extremely localized areas, it is important that laser parameters be controlled to minimize the heat-affected zone (HAZ).[9].

Nowadays, LST is one of the most innovative techniques in the industry. Despite its high cost, the manufacturer prefers to use laser technology due to the development of new types of lasers and the strict criteria for producing high added value parts. The final polishing process, which has a high added value and is manually carried out by skilled employees, can account for up to 30% of the entire production cost for the manufacture of dies and molds. Ukar et al. conducted laser Polishing on DIN 1,2379 tool steel tests using CO_2 and High-Power Diode Lasers (HPDL). The laser polishing parameters as well as its level of influence on the melted surface have been specified using experiments and the Design of Experiments (DoE) techniques. Results showed that to it is possible to obtain 80% final roughness reduction compared to the initial roughness value [10].

A different technique was preferred in another study to evaluate the surface topography of laser-polished surfaces on ball-machined semi-finished parts of 1.2379 tool steel. The method is based on estimating the laser thermal field. In the tests, a 3.1 KW diode laser was utilized. Experimental verification demonstrates a reasonably good agreement between estimated and measured average roughness (Ra) and average roughness depth (Rz), with errors of less than 15% in all settings [11].

Andre et al. [12] contributed to enhancing and expanding the empirical data set for laser micro polishing of 1.2379 tool steel by using a diode-pumped Yb:YAG disk laser . The results reveal that to obtain larger laser beam sizes, smaller laser polishing fluids are required. Furthermore, with larger laser beam diameters, the same or lower surface

roughness and less undesired surface characteristics are formed. This demonstrates a possible way for industrial laser micro polishing applications, where area rates of up to a few m^2/min may be produced using commercially available laser beam sources [12].

In the literature there are limited studies on laser surface treatment of 1.2379 and they used CO_2 and diode laser, there are no studies which use fiber laser in the treatment of 1.2379 tool steel. In this thesis, laser surface treatment process applied on 1.2379 cold work tool steel with variant laser parameters (i.e. power, pulse duration, frequency and line spacing). Following that, hardness and roughness values of treated surfaces were measured. Additionally, this research aimed to determine optimum laser parameters for roughness and hardness by using different regression models and optimization techniques.

1.2. Objectives of Thesis

Laser surface treatment is one of the important operations for material processing. It gives an opportunity to change the mechanical properties of cold work tool steel. Compared to other methods which are used for surface treatment process, laser surface treatment has many advantages such as low cost and compatibility to automation.

In this thesis, 1.2379 cold work tool steel which is mostly used material in die and mold industry is treated with fiber laser to improve surface properties. In the industry the hardness and roughness of this material plays an important role in manufacturing. Thus, with LST process surface properties were modified. In order to determine proper laser parameters for 1.2379 cold work tool steel, three main processes were performed in this study. In the first stage, the surface of the material was processed with a laser and the hardness and roughness values were measured. In the second stage, regression models were created and the best model was selected. In the final stage, four different non-traditional optimization methods which are Random Search, Simulated Annealing, Differential Evolution and Nelder-Mead were performed to find optimum roughness and hardness values. The following are some of the key reasons for writing this thesis:

- To treat the surface of 1.2379 cold work tool steel by using low power fiber laser
- To investigate the effect of laser parameters (i.e., power, frequency, scan speed and line spacing) on surface properties such as hardness and roughness of 1.2379 cold work tool steel

- Improving the surface quality of 1.2379 cold work tool steel for long-term use.
- Decreasing the set-up number by increasing the tool life in mass production.
- Observing different regression methods and finding the high R^2 value.
- To consider proper laser parameters for expected hardness and roughness values by using optimization methods.

As a summary, the flowchart of LST optimization of 1.2379 cold work tool steel is given in Figure 1.2.

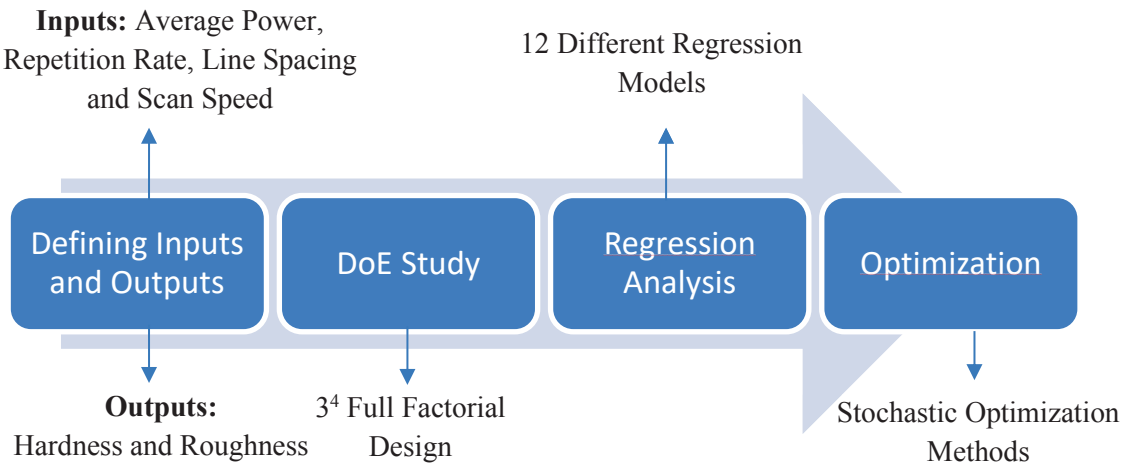

Figure 1.2. Flow chart of LST optimization for 1.2379 cold work tool steel

CHAPTER 2

LASER TECHOLOGY AND APPLICATIONS

2.1. Lasers

The foundations of the laser system were first laid in 1917 by Albert EINSTEIN with the concept of “stimulated emission” predicted using a mathematical proof [3]. The first ruby laser was introduced in 1960, and soon after that, systematic research on laser-material interactions rapidly expanded. With the ruby laser, it has been found that the special interaction between the laser beam and the material causes permanent changes to the mechanical properties of material [13].

The meaning of LASER word is light amplification by stimulated emission of radiation [14]. A laser is composed of three parts: an energy source ('pump') a lasing medium (solid, liquid or gas), and an optical resonator as shown Figure 2.1. This establishes the required circumstances for photons to be stimulated and amplified by a cascade effect to produce laser light. Compared to other light sources, lasers have a high power density which allows them to generate a highly focused source of intense heat that declines only little with distance from the source[15].

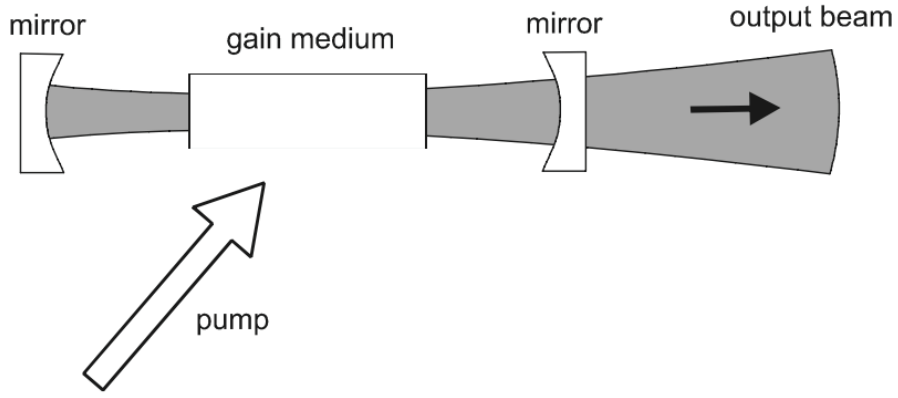

Figure 2.1. Basic components of a laser system [16]

In practice, a laser device consists of a medium decoupled between two mirrors, a fully reflective mirror (fully glazed) on one side and a partially reflective mirror (semi-glazed) on the other side. When this medium is pumped in such a way that a localization

transformation occurs that raises the majority of the active atoms (or molecules) in it to higher than normal energy levels, a coherent light that can reflect back and forth between the end mirrors of the cavity occurs. This situation leads to the fact that the level of this coherent light reaches a threshold point (the point at which the gain generated by light amplification begins to exceed all the losses that can occur simultaneously). In this way, the device begins to emit a beam of laser light [17] as shown in Figure 2.2 [18].

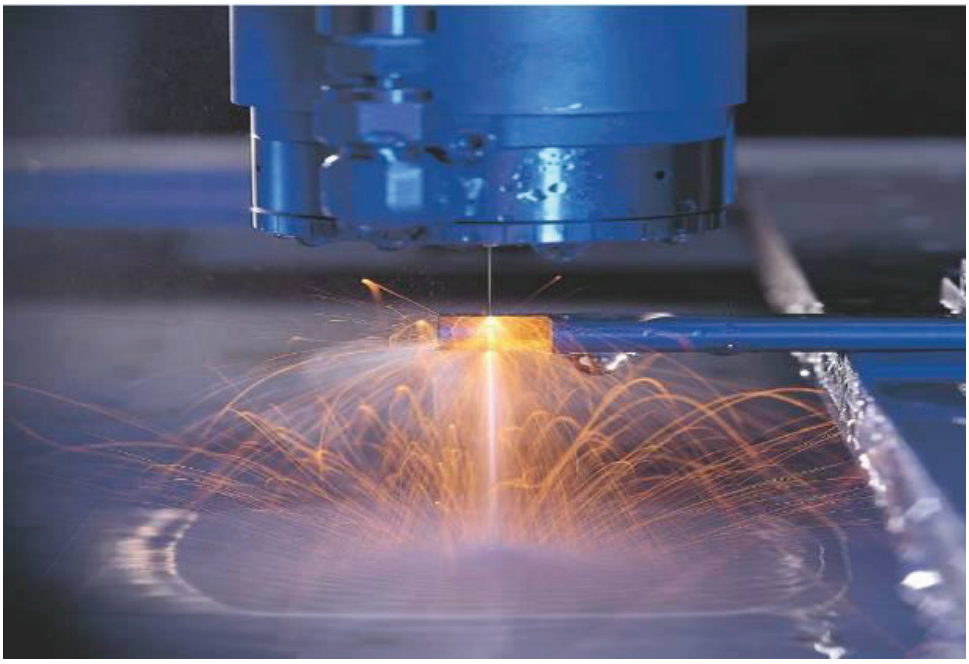

Figure 2.2. Light emitted by the laser nozzle [18]

From an engineering point of view, a laser is an energy conversion device that simply converts the energy coming from a primary source (optical, chemical, electrical, thermal or nuclear) into an electromagnetic beam (ultraviolet, visible or infrared) of a special frequency. This transformation is achieved with certain solid, liquid or gaseous media. When these media are excited with certain techniques at the molecular or atomic scale, a coherent and relatively monochromatic (almost single frequency) form of light (a laser light beam) is formed. Due to their coherence and monochromaticity, both low-power and high-power laser light beams have a very small divergence angle. For this reason, they can be transmitted relatively up to extremely large distances either through transmissive or reflective type focusing lenses [17].

2.2. Laser Classification

There are various types of lasers, and they can be classified based on the pump mechanism and the composition of the energy levels. Although additional sources of energy such as nuclear, chemical or particle-kinetic energy are potential, the most commonly used pumping processes are optical and electrical. The energy levels might be either electronic (describing distinct energy states of an electron), vibrational (describing different energy states of atomic vibrations in a solid), or a mix of them [16]. Figure 2.3 shows the main types of lasers developed and still in use from the past to the present, categorized according to the environment in which they are produced [19].

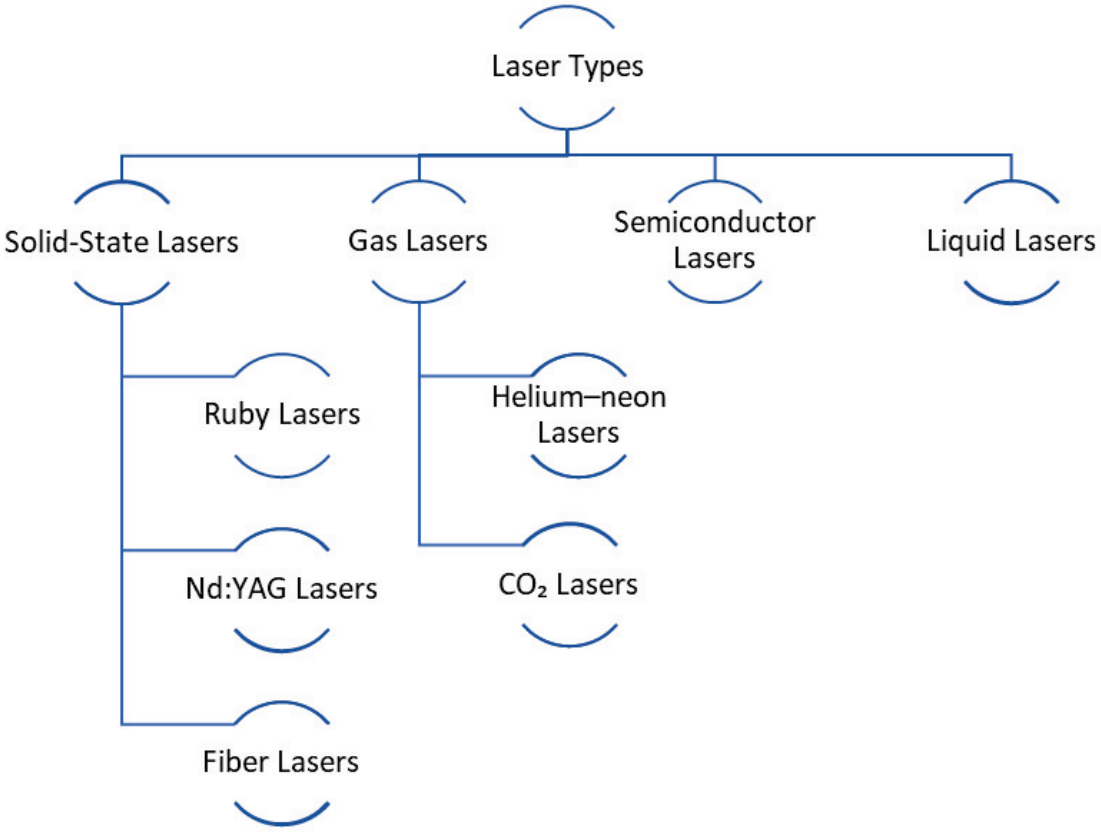

Figure 2.3. Main laser types

2.2.1. Solid-State Lasers

Ruby laser was the first solid-state laser. Ruby is an aluminum crystalline and this crystalline involves some amount of chromium. These chromium atoms generate a red laser beam [20].

The usage area of solid-state lasers has grown significantly since the invention of another solid-state laser which is called Nd: YAG. In this laser, cylindrical rod-shaped crystals are coated with an antireflective material and polished on both ends. The crystals are held together by a metal container. Special flash bulbs and reflecting mirrors are inserted in the container depending on the stimulation type used. A laser beam with a wavelength of 1064nm is produced when a Nd:YAG crystal is excited by a high intensity light [21].

2.2.1.1. Fiber Lasers

With the development of fiber optic components, laser science enhances its fundamental parameters such as average power, pulse energy, peak power, wavelength and pulse energy characterization. Nowadays, fiber lasers are the most recent generation of laser technology. The fundamental loss of fused silica fibers has now been reduced to 0.15 dB/km at 1550 nm. Due to its advantages such as, good beam quality, high brightness, low noise, low cost, high power, extended lifetime, high reliability and minimal maintenance need, fiber laser technology has evolved from a laboratory instrument to a highly welcome industrial solution. Because of their adaptability, fiber laser systems have found a wide range of applications in everyday technical practice [22,23].

2.2.2. Gas Lasers

By inducing gaseous substances, gas lasers generate a laser beam. These compounds are inserted and fixed in a closed tube and the laser beam is activated by electrodes located throughout the tube. The gas composition changes depending on the laser type that is used. The early gas lasers employed a combination of helium and neon. Recent studies on the gas combination have indicated that CO_2 laser mixtures are more efficient than helium and neon lasers. Owing to the wavelength of the laser beam they

generate and their great power capacity, these lasers are commonly employed in industrial operations (up to 50 kW) [20]. Over time, most of the work has turned to new closed-type lasers that do not require gas supply during operation. These lasers have a more compact construction and lower running costs than CO_2 lasers that require gas supply. The heat generated in the closed laser tube is transported to the exterior surfaces by the mixed gas. CO_2 lasers are commonly utilized in the treatment of plastic materials [24].

2.2.3. Semi-Conductor Lasers

Semi-conductor laser is created using crystals produced from semiconductor materials. A semiconductor substance is a gallium arsenide crystal. In this form of crystal laser, electrons lose energy and produce photons when a positive voltage is applied to the "p" side and a negative voltage is applied to the "n" side of the combination surface of "p" and "n" type materials. This photon-electron collision produces additional photons. Laser beams are formed as a result of photons reaching a sufficient level. These lasers generate a significant amount of light. Semi-conductive lasers provide a higher than 50% efficiency. The wavelength and optical properties of a laser beam produced by a diode laser are widely used in industry, metal and plastic materials welding, and a variety of surface treatments such as surface cleaning and hardening [25,26].

2.2.4. Liquid Lasers

There is a substantial risk of damage while working with solid lasers owing to heat created in the material during high-power operation or heat caused by the pumping light. Instead of a crystalline or glassy rod, organic dyes are deposited in solutions created by reducing them in solvents in liquid lasers. The most distinguishing factor from the others is that the desired wavelength may be investigated by modifying it in a specific spectrum based on the material employed rather than a single wavelength[27,28].

2.3. Applications of Lasers

Lasers have been used in our daily lives since the 1970s, thanks to rapidly developing technology. Lasers, which are classified as low-intensity lasers or high-intensity, have a highly diverse and broad range of applications. Based on the main categories, the application areas of lasers used for industrial and commercial purposes can be represented in Figure 2.4. There are also numerous key scientific applications being explored on various scales by government and industry groups, as well as universities, such as laser weapons, laser-induced nuclear fusion, isotope enrichment, spectroscopy and atomic physics, and measurement.[18].

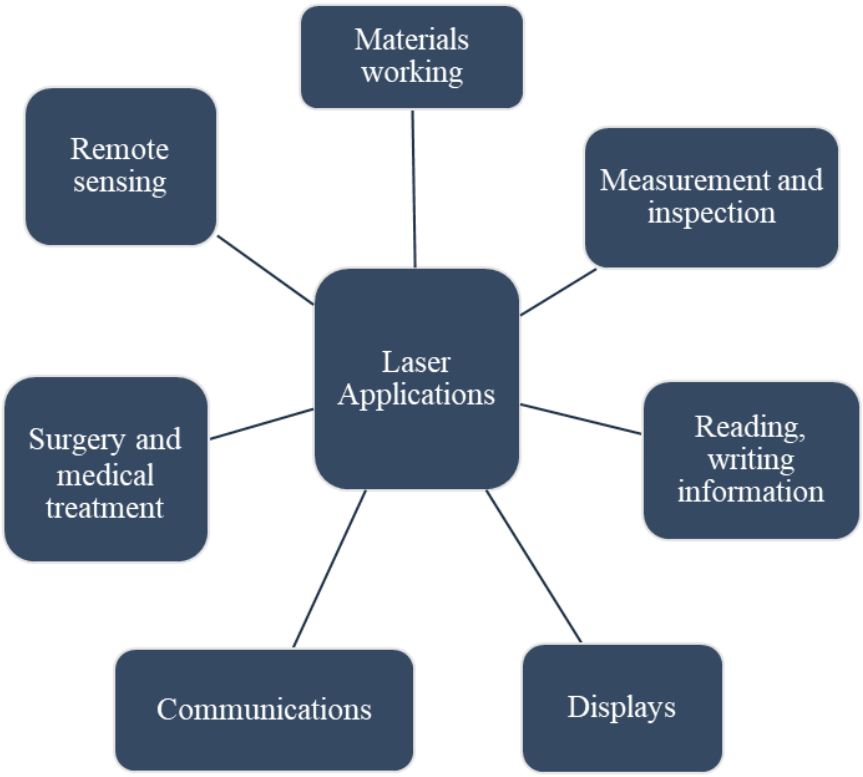

Figure 2.4. Laser applications

2.4. Laser Material Interaction

Nowadays, laser material interaction is one of the fastest-growing fields, and its advancement has paralleled the development of novel laser system designs. Compared to conventional methods, laser material processing offers various advantages. Processing

materials with lasers became increasingly significant after the introduction of new laser types and progress in applied sciences and industry [3]. Modifications in the crystal structure, chemistry, and morphology of the material induced by laser radiation causes changes in the material's behavior. The laser capacity to deliver large amounts of energy to the material in a very short period of time at a region near to the surface enables to change in the material properties [29]. The capacity to precisely manage where in the material and at what rate energy is deposited is one of the laser's important features as a material processing tool. To accomplish the required material modification, this control is performed through the right selection of laser processing settings[30].

2.5. Laser Surface Treatment

The selective heat treatment of metallic materials for decreased wear was one of the earliest commercial uses for laser surface treatment process [31]. Heat treatment of metals has typically employed heating to a specific temperature in an oven, flame, induction, or electric arc to create a crystal phase change and then rapidly cooling to ambient temperature and freezing in a non-equilibrium phase. The pace of cooling from the high temperature crystal phase impacts the shape and mechanical characteristics of the subsequent room-temperature crystal. Such heat treatments are widely employed to harden or temper load-bearing surfaces in order to minimize friction, wear and working life [32]. However, machining the entire part is undesirable in most circumstances because it makes the part prone to degradation or fracture. Rapid surface heating with reduced thermal penetration is partly owing to the laser. Following, self-quenching into the cooling mass change is restricted to a thin layer of surface material. By changing laser parameters such as pulse duration (or scan speed for CW lasers) and intensity, the heating and quenching rates, and hence the resultant material characteristics can be modified [33]. High processing rates, accurate curing depth control, reduced component deformation and cracking, elimination of separate quenching media, and selective hardening of small hard-to-reach places are the primary benefits of laser surface heat treatment [30].

LST applications can be grouped into two types. The first one is to remanufacture or refurbish parts in order to recover their qualities and dimensions [34]. The second one is to create new materials with superior characteristics. Table 2.1 lists several articles that used the LST process.

Table 2.1. Some applications of LST [35–43]

Material	Application	Improvement	References
CMSX-4 (Ni-based super alloy)	Repair of turbine blades	This method helped to develop monocrystalline CMSX-4	[35]
Stellite-6/WC on B27 boron steel	Repair of tools for soil cultivation	Formation of intermetallic compounds improved the wear resistance	[36]
NI40 and NI60 on C60 steel	Improvement of barrel- screw system in plastic injection molding	Ni-Cr alloy clad improved the microhardness	[37]
CPM9V steel on H13 tool steel	Repair of molds and dies used in hot and cold working	Presence of compressive stress due to formation of martensite phase	[38]
Grade C wheel U75V rail with 316L, 420, 410	Repair of damaged railway wheels	The wear rates decrease with increased hardness of the clad materials	[39]
Titanium hydroxylapatite on Nitinol	Coating on Nitinol implants to restrict nickel release	Modulus of elasticity of coated samples falls in the range of 6–30 GPa which is similar to the natural bone	[40]
Mg-Zn-Dy alloy casted and laser melted	Restrict in vitro degradation and improve tissue integration	Improvement in in vitro degradation due to formation of insoluble protective layer	[41]
Powdered Co29Cr9W3Cu alloy	SLM is used to develop Co29Cr9W3Cu alloy joint prostheses	Initiation of crack is arrested due to plastic deformation caused by strain-induced martensitic transformation	[42]
Ti powder on Ti6Al4V substrate	Improve in vitro biocompatibility capacity of the titanium deposits to be used as medical implants	In vitro test of samples in Hank's solution shows that the leaching was within the desired values	[43]

CHAPTER 3

MODELING

3.1. Design of Experiment (DoE)

Design of Experiment (DoE) is a useful approach to discover new processes as well as learning more about current processes, and then selecting these processes to obtain world-class performance. Ronald Fisher invented the first DoE in the early 1920s. His first research included assessing the effect of different fertilizers on different plots. The eventual stage of the crop was determined not just by the fertilizer, but also by a variety of additional elements. Fisher employed DoE to isolate the influence of fertilizer from the effects of other variables. DoE has been extensively recognized and used in biological and agricultural domains after this study. It is known that several DoE study have been effectively employed by many US and European companies in the last 15 years [44].

DoE is a very successful statistical and mathematical method for improving the performance of a system or process, which is defined as the conversion of inputs into outputs. Factors or variables, levels, and responses are the components of the experimental approach's design. The process's input variables can be controllable and uncontrolled factors [44,45]. The potential applications of DoE in manufacturing processes include:

- improved process yield and stability
- improved profits and return on investment
- improved process capability
- reduced process variability and hence better product performance consistency
- reduced manufacturing costs
- reduced process design and development time
- heightened engineers' morale with success in solving chronic problems
- increased understanding of the relationship between key process inputs and output(s)
- increased business profitability by reducing scrap rate, defect rate, rework, retest, etc. [46]

The appropriate DoE technique should be carefully selected according to the goal of the experiment and number of factors. There are many methods used in DoE study, widely used ones listed in this literature review. These methods are Full Factorial, Randomized Complete Block Design, Fractional Factorial, Taguchi and D-Optimal Design [47,48].

3.1.1. Full Factorial Design

Full and fractional factorial designs at two and three levels are well known and most widely used DoE techniques by manufacturing industries. Using factorial designs, a researcher can obtain a consistent response on the effects of variables. There are two kinds of factorial designs, these are full and fractional factorials. A full factorial design is an experimental design in which every factor setting interacts with every other one. When there are five or more components, the complete factorial design needs a substantial amount of operation and is inconvenient. In such instances, fractional factorial design can be preferred [44,49].

3.1.2. Randomized Complete Block Design

The randomized complete block design (RCBD) is a typical design for biostatistical research in which comparable experimental units are divided into blocks or replicates. It is used to control variance in an experiment by, for example, accounting for geographic effects in a field or greenhouse. The RCBD is distinguished by the fact that each block receives each treatment exactly once. Randomized complete block designs differ from completely randomized designs in that the experimental units are divided into blocks based on known or hypothesized variance that is separated by the blocks. Variation like fertility, sand and wind gradients, or animal age and litter may be separated using proper blocking. As a result, the circumstances within each block are as uniform as feasible, yet considerable variances may occur between blocks [50].

3.1.3. Fractional Factorial Design

In full factorial experiment design, combinations of all levels of factors are examined one by one, which increases the cost of the experiment and takes a lot of time. In other words, the design of a full factorial experiment has a maximum duration and expense. The correlation between the data obtained from the experiment and the cost and time spent is very critical in the design process. In order to save cost and time, fractional factorial experiment design reduce the number of experiments [51].

3.1.4. Taguchi Design

Taguchi experimental design approach is used as an efficient method for solving optimization problems by minimizing processing performance with the least tests and at the lowest cost. In this method, it is expected to save time and money by minimizing the number of experiments by employing the vertical indexes of the Taguchi method [52].

In Taguchi technique, all elements influencing process quality can be classified into two categories: control factors and noise factors. The control variables are defined by the manufacturer and are simply adjustable. These are the most significant criteria in establishing the quality of product properties. The Taguchi method is applied in the following steps:

i. identifying the factors/interactions,
ii. identifying the levels of each factor,
iii. selecting an appropriate orthogonal array (OA),
iv. assigning the factors/interactions to columns of the OA,
v. conducting the experiments,
vi. analyzing the data and determining the optimal levels,
vii. conducting the confirmation experiment[53].

3.1.5. Optimal Design (D-Optimal)

D-optimal design, which is a kind of computer-aided design, complies with the high-level standards or criteria specified by the developers in the development stage. The product prototype generates very close results in this design method and usually appears

to approach the perfect design for that product. D-optimal designs are flat optimizations that are based on the optimality criterion and model to fit. D-optimal design matrices are typically not orthogonal, and the effect estimates are coupled, in contrast to normal classical designs such as factorization and fractional factorization. D-optimal design provides various advantages in terms of time and cost limitations. This method directly focusses on particular criteria and reduces the costs associated with the investigation process. Different factors allow us to create unique combinations. Shortly, this method prefer to use more promising combinations while ignores insignificant results [44,47,49,54].

3.1.6. Box-Behnken Design

Box-Bhenken design was created by Box and Bhenken in 1980. This experimental design is a practical method to develop second order response surface[55]. The Box-Behnken Design generates an experimental matrix that is required for the combination of process parameters and conditions[56]. Box Bhenken is one of the important experiment design methods that allows to reduce experiment costs. With the use of progressive regression analysis, Box-Behnken experimental design results can be predicted in a short time by conducting a small number of experimental studies[57].

3.2. Regression Analysis

Regression analysis is one of the most important subjects of statistics. Regression analysis is a mathematical analysis technique created to predict or estimate the relationship between two or more variables that have a cause-effect relationship [58].

Generally, a regression model is expressed by Equation 3.1 (y represents the dependent variable, α represents the constant, x_1 represents independent variable, β1 indicates the (regression) coefficient of the independent variable x and the e denotes the error (or residual) of the equation) .The steps of regression analysis is shown in Figure 3.1 [59].

$$y = \alpha + \beta_1 x_1 + e \quad \textbf{(3.1)}$$

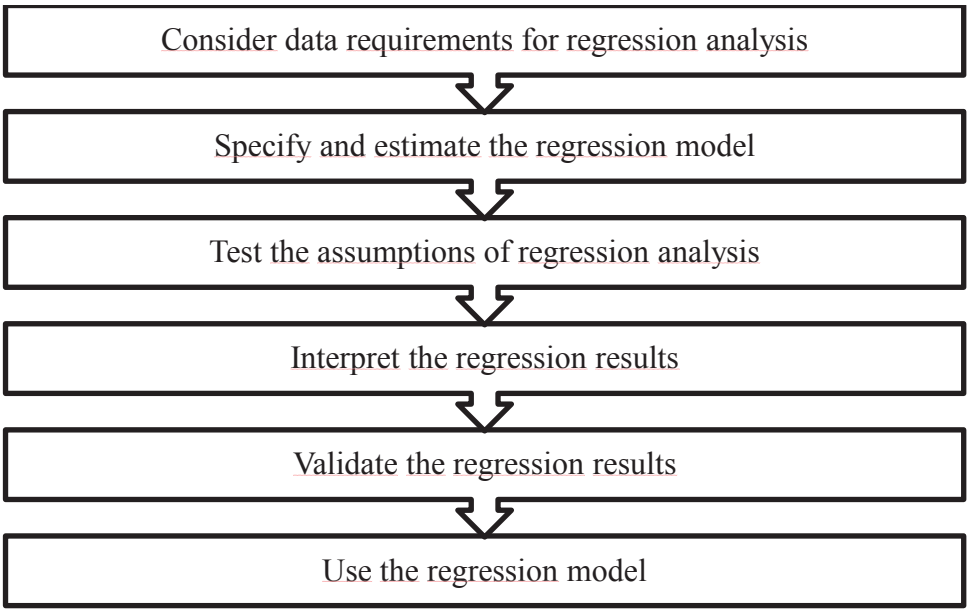

Figure 3.1. Steps of regression analysis

3.2.1. Simple Linear Regression

Simple linear regression describes the relationship between the response variable Y and the given input variable X [60]. While correlation and its related inference can assist in determining the relationship between two quantitative variables, they do not provide the full picture. While the correlations between two sets of predictor and responder may be comparable, the effect sizes are chosen differently. A more detailed view of the relationship between predictor and response is provided by simple linear regression. By establishing a few assumptions about the error that surrounds our regression line, we can choose the best line to describe this relationship, one that is directly related to the correlation [61].

The simple linear regression relationship for response variable Y and the input variable X can be represented by Equation 3.2. In the given equation β_0 and β_1 are unknown parameters and can be predicted from data. Also e represent the random error of the regression model [62,63].

$$Y = \beta_0 + \beta_1 X + e \quad \textbf{(3.2)}$$

3.2.2. Simple Non-linear Regression

The linear model produces good outcomes in many scenarios; however, this may not be possible in other cases. The relationship between response and input variable cannot always be expressed with the use of the linear model. Therefore, nonlinear models can produce more accurate findings as an alternative way [64]. Simple non-linear regression model can be expressed by Equation 3.3 [63].

$$Y = \beta_0 + \beta_1 X^2 + e \quad \textbf{(3.3)}$$

3.2.3. Multiple Linear Regression

Simple linear regression models just one variable uses to explain variation of Y data, while more than one variable uses in multiple regression models to determine the variation of Y data. Multiple Regression is used to describe regression with more than one X variable. The relation Multiple linear regression model can be expressed by Equation 3.4 which has n explanatory (X) variables:[65]

$$Y = \beta_0 + \beta_1 X_1 + \beta_2 X_2 + \cdots + \beta_n X_n + e \quad \textbf{(3.4)}$$

3.2.4. Multiple Non-linear Regression

Multiple nonlinear regression is a kind of regression analysis in which the relationship between observation data and a function may be specified. In the multiple nonlinear regression model, the dependent variable is determined by various independent variables through nonlinear combinations[66]. Multiple non-linear regression model can be shown by Equation 3.5 [63].

$$Y = \beta_0 + \beta_1 X_1 + \beta_2 X_2^2 + \cdots + \beta_n X_n^n + e \quad \textbf{(3.5)}$$

3.3. Coefficient of Determination (R^2)

The coefficient of determination is the percentage ratio of total variability in the dependent variable accounted for by the regression equation in the independent variable (s). A R^2 value of 1 implies that the fitted regression equation accounts for all the variability in the dependent possible values in the sample data. The number of 0 for R^2 shows that the regression equation explains for none of the variability[67].

After fitting the regression model, checking whether the model is sufficient or not is the most important part of regression analysis. It is necessary to guarantee that the generated model is sufficiently close to the correct model and to check whether it provides all the assumptions of the least squares regression analysis. If the regression model does not provide sufficient adaptation, it will give weak or misleading results[58].

The Coefficient of Determination, also known as the R-squared (R^2), is the most widely used statistic in regression. The R^2 is the fraction of data variance (Y) explained by the model (X). The R^2 is determined by Equation 3.6. Figure 3.2 shows how the R^2 is the proportion of variation in the data (Y) explained by the model [65] .

$$R^2 = \frac{SSM}{SST} = 1 - \frac{SSE}{SST} \quad \textbf{(3.6)}$$

$$SSE = \sum_i (\hat{y}_i - \bar{y})^2 \quad \textbf{(3.7)}$$

$$SST = \sum_i (y_i - \bar{y})^2 \quad \textbf{(3.8)}$$

Where;

Sum of Squares Total:

SST is the Variation in the data also known as the difference between data and overall Avarage

Sum of Squares Model:

SSM: Variaion of the model or the difference between average and estimated data

SSE is Sum of Squared Regression also known as variation not accounted by the model

$\boldsymbol{y_i}$ is the y value for observation i

$\bar{\boldsymbol{y}}$ is the mean of y value

$\hat{\boldsymbol{y}}_{\boldsymbol{i}}$ is the predicted value of y for observation i

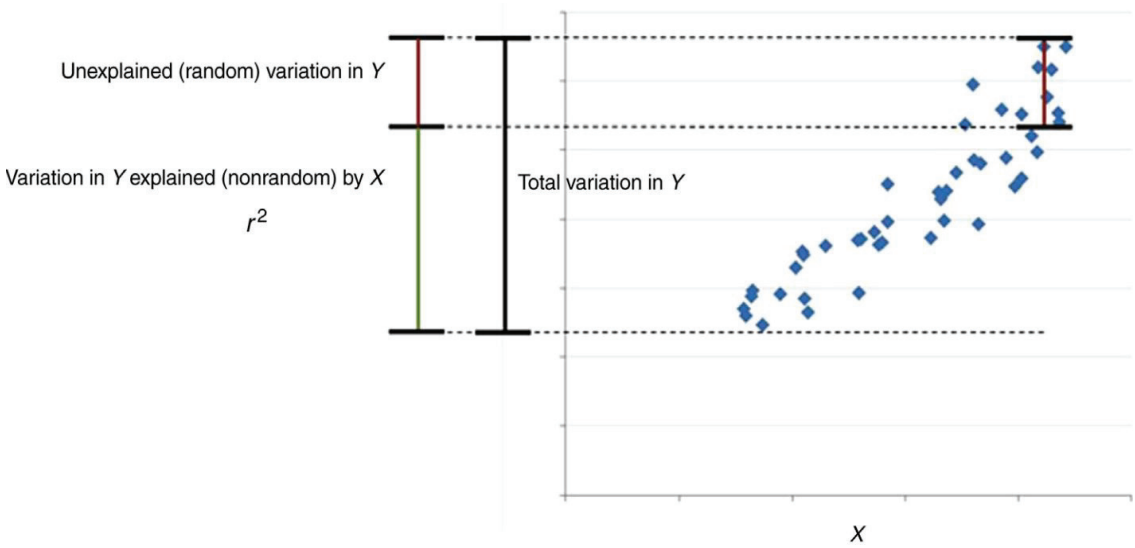

Figure 3.2. How the R^2 is the proportion of variation in the data (Y) explained by the model[65]

The adjusted R-squared analyses the explanatory power of regression models with different predictor values. The adjusted R-squared is a variant of R-squared that has been changed to account for the number of predictors in the model. Only if the additional term enhances the model more than could be predicted by chance does the adjusted R-squared rise. It falls when a predictor improves the model by a less amount than would be anticipated by chance. It is possible for the adjusted R-squared to be negative, although it is generally not. Also, It is never greater than R-squared [68]. Adjusted R^2 can be calculated by using Equation 3.9 [69]:

$$R^2_{adjusted} = 1 - \frac{(1-R^2)(n-1)}{n-k-1} \quad \textbf{(3.9)}$$

Where N is the sample size, and k is the number of predictor variables in the analysis. Smaller values for N, and larger values for k, lead to greater downward adjustment of R^2.

3.4. Neuro-Regression Modeling

Artificial neural networks and regression analysis are two main data analysis techniques. Both approaches have their advantages and disadvantages. In order to build more reliable models and predictions, a hybrid technique was developed to combine the

advantages of these two methods while minimizing their limitations. This method is known as Neuro-Regression. The suggested technique combines the benefits of the RA and ANN methods while avoiding their disadvantages, resulting in a substantially reduced error rate when compared to both methods. The primary objective of neuro-regression research is to develop a learning model that can reliably estimate previously unknown data. As a result, the learning model developed must be generalized in order to ensure the right categorization of data in the future. Generalization relates to how successfully the model learns from the provided data and applies what it has learnt. Validation, Training, and Test sets are the most often utilized methodologies for measuring generalization. If the model performs well on data that it has not observed in training, it is considered to perform well on the provided data [47,70].

3.4.1. Train and Test Set

The data collection should be separated into test and training sets before conducting mathematical modelling. This divide might be around 80% training dataset and 20% testing data. The training set is the dataset used to train the model. The test set is a data set that is used to evaluate the model that was created in the training set. The model is first trained on the training set before making predictions on the test set. Following that, the predictions are compared with the real response variable in the test data, and the model's accuracy is assessed. Furthermore, the model learns better when the training set is larger [47,70].

3.4.2. Validation Set

After the model is decided at the end of each training with the validation set, it is tested with the test set and the effectiveness of the model is observed in a more reliable way. The validation set has no influence on the model's fit performance. Furthermore, the test set determines whether the model is under or over fit. Only overfitting to the test set is checked by the validation set [70,71].

CHAPTER 4

OPTIMIZATION

The process of obtaining the best possible result under specified conditions is known as optimization. Engineers must make various technological and operational decisions at various phases of the design, development, and maintenance of any engineering system. All of these options are ultimately aimed at either minimizing the work required or maximizing the intended result. Because the effort needed or expected utility in each practical scenario may be described as a function of specific selection factors, optimization can be defined as the method of determining the parameters that give a function the highest or smallest value [72].

Performance optimization is a critical subject in the design and operation of modern engineering systems in a wide range of sectors such as manufacturing, robotics, communication and logistics. Most engineering systems are either too complex to model or the system parameters are difficult to identify. Because of these reasons learning methods must be employed [73].

4.1. Single Objective Optimization

The maximum or minimization of the objective function based on a single variable under a constraint or an unconstrained problem is the subject of single-objective optimization problems. The objective function in single-objective optimization problems has just a single variable. The function might change depending on the various values of that variable.

The single-objective optimization function can have:

a. relative / local min
b. relative / local max
c. absolute / global min
d. absolute / global max.

Single-objective optimization is a useful method in less complicated real-time studies. However, optimization is also required at low levels [74]. The mathematical definition of single objective optimization can be expressed as follows:

Minimize f (x) or Maximize f (x)

where, $x = (x_1, x_2, x_3, \ldots, x_n)^T$

Subject to,

$g_i(x) \leq 0 \qquad i = 1,2,\ldots,m$

$h_j(x) = 0 \qquad j = 1,2,\ldots,k$

4.2. Multi Objective Optimization

Multi objective optimization (multi objective programming or multicriteria optimization), is a branch of multiple-criteria decision-making that deals with mathematical optimization problems where numerous objective functions must be simultaneously optimized. Numerous scientific disciplines, including engineering, have used multi-objective optimization to help make the best choices when multiple objectives must be compromised [75]. The mathematical definition of multi objective optimization can be expressed as follows:

Minimize $f_1(x), f_2(x),\ldots,f_r(x)$ or Maximize $f_1(x), f_2(x),\ldots,f_r(x)$

where $x = (x_1, x_2, x_3, \ldots, x_n)^T$

Subject to,

$g_i(x) \leq 0 \qquad i = 1,2,\ldots,m$

$h_j(x) = 0 \qquad j = 1,2,\ldots,k$

4.3. Traditional and Non-Traditional Optimization

Traditional and non-traditional techniques are the main categories of optimization methods. Traditional and non-traditional optimization are also called deterministic and stochastic optimization respectively. These methods have advantages and disadvantages based on usage areas. The traditional approach begins with the initial answer and develops the ideal solution with each further iteration. The decision about the first strategy will affect this convergence. These techniques are inappropriate for discontinuous objectives. Because of this, the necessity of non-traditional methods arises. Also, certain unconventional techniques are referred to as nature-inspired techniques[76].

Traditional techniques are slower than non-traditional techniques, however if the problem is small more accurate results can be found. Mathematical programming,

Dynamic programming, Integer programming are some of the traditional optimization techniques. Non-Traditional Optimization techniques are fast enough, however there is no guarantee for optimum solution like traditional techniques. It is kind of approximation method. [77].

Non-traditional optimization methods are used in various studies in literature in recent years and scientists continue to develop new strategies and approaches in stochastic optimization techniques. Some of the example of stochastic optimization methods are; Simulated Annealing (SA), Genetic Algorithm (GA), Differential Evolution (DE), Random Search (RS), Particle Swarm Optimization (PSO), Tabu Search (TS), Artificial Bee Colony (ABC), Ant Colony Optimization (ACO), Markov Chain Monte Carlo (MCMC), Harmony Search (HS), Covariance Matrix Adaption (CMA), Grenade Explosion Method (GEM). Since laser surface treatment process is extremely nonlinear, stochastic optimization methods were preferred. Four different optimization methods (Simulated Annealing (MSA), Differential Evolution (MDE), Nelder-Mead (MNM) and Random Search (MRS)) were preferred for this thesis.

CHAPTER 5

MATERIAL AND METHODS

In this chapter, the material and techniques utilized in the experiments are discussed in detail.

5.1. Material

The material employed in this study is 1.2379 cold work tool steel. The following chapters include full details about tool steels.

5.1.1. Tool Steel

Any steel that is "used to create tools for cutting, molding, or otherwise shaping a material into a part or component appropriate to a certain function" is called as a "tool steel"[78]. Tool steels are high-alloy steels that shape, mould and cut other materials, such as steels, nonferrous metals, and polymers used in the manufacturing of tools, dies, and molds. Tool steels can be hardened and tempered and can be either carbon, alloy, or high-speed steels. To suit specific criteria, they are often melted in electric furnaces and manufactured using tool steel techniques. They can be incorporated into certain hand tools or mechanical fixtures to cut, shape, mold and blank materials at normal or high temperatures. In a wide range of other applications where resistance to wear, strength, toughness, and other qualities are required for optimum performance, tool steels are also used [79].

The American Society for Testing and Materials (ASTM) designation, in which each steel grade is called by a letter followed by a number, is one of the primary classification techniques for tool steels. The number, which is often in sequential (and typically historical) sequence, designates a certain developed steel, while the letter indicates one feature of the tool steel. According to ASTM, tool steels are classified into nine types of steels. Table 5.1 presents the symbols for the tool steels in the ASTM group[80].

Table 5.1. ASTM classification of tool steels

Classification ASTM	Symbol
Water-hardening tool steels	W
Shock-resisting tool steels	S
Oil-hardening cold work tool steels	O
Air-hardening, medium-alloy cold work tool steels	A
High-carbon, high-chromium cold work tool steels for Dies	D
Plastic mold steels	P
Hot work tool steels, chromium, tungsten	H
Tungsten high-speed tool steels	T
Molybdenum high-speed tool steels	M

5.1.1.1.Cold Work Tool Steel

In the industry, various metal forming processes such as pressing, bending, pulling, cutting and punching of workpieces are performed by cold work molds. The main parts that directly contact and shape the workpieces in these molds are cold work tool steels. For this reason, the correct selection and processing of mold steels takes a critical role in the durability of molds. Cold work tool steels are usually used in forming process of the formed material at temperatures below 200°C [79,81].

The cold-work tool steels classify into four main groups: the O-series (oil-hardening), W-series (water-hardening) the A-series (air-hardening), and the D-series (high carbon-chromium)[82].

5.1.1.1.1. 1.2379 Cold Work Tool Steel

1.2379 (AISI D2), a ledeburitic chromium rich steel with 1.55% C, is one of the most extensively used cold work tool steels in mould and die applications [83]. This steel has been highly preferred in critical applications in industrial sectors such as forming dies, collets and gauges in recent years. 1.2379 cold work tool steels are used as dies, trimming dies, coining dies, punches, shear blades, fuller, phillips head forming dies, thermosetting resin forming dies, cold forming dies, thread rolls, fine blanking, stripper plates, profiling

rollers and press tools, brick moulds, chisels, pneumatic tools, etc. [84–87]. The worldwide demand for steel is expected to increase from 1700 million tons to almost 1750 million tons between 2016 and 2018, as indicated in Figure 5.1**.** Additionally, the growth in the production of passenger cars will definitely have a positive effect on the tool and mold industries. The chemical composition of 1.2379 cold work tool steel is given in Table 5.2.

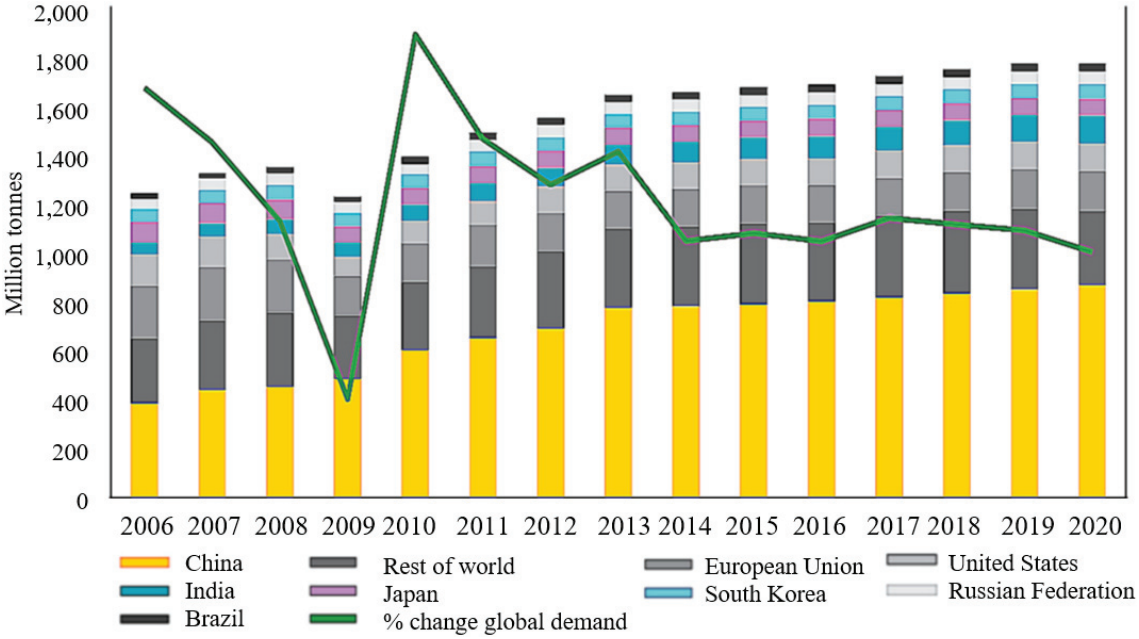

Figure 5.1. Global steel consumption 2006–2020[83]

Table 5. 2. The chemical composition of 1.2379 (D2) cold work tool steel (%) [88]

Fe	Cr	C	V	Mo	Mn	Si
~84.1	11.86	1.56	0.84	0.83	0.38	0.4

5.2. Experimental Methods

The experimental study was performed on 1.2379 cold work tool steel with a cube which dimensions are 30 mm × 30 mm × 60 mm. Firstly, the samples were cleaned by an ultrasonic bath in acetone solution at 50 ° for 4 minutes as shown in Figure 5.2. After that samples were sandpapered as seen in Figure 5.3**.**

Figure 5.2. Ultrasonic bath

Figure 5.3. Grinding and polishing machine

Four main laser parameters (average power, repetition rate, scan speed and line spacing) are used as input and the surface properties such as hardness and roughness specified as output parameters as shown in Figure 5.4. The range of laser parameters

specified according to pre-experimental studies. To increase accuracy of optimization process full factorial design was applied by using four factors (average power, repetition rate, scan speed and line spacing) in 3 levels and two responses (hardness and roughness). To create design of experiment (DoE) data commercially available Design-Expert software was used. The building information is shown in Table 5.3. and 3^4 full factorial DoE data is given in Table 5.4. By using four factors and three levels, 81 experimental runs were created.

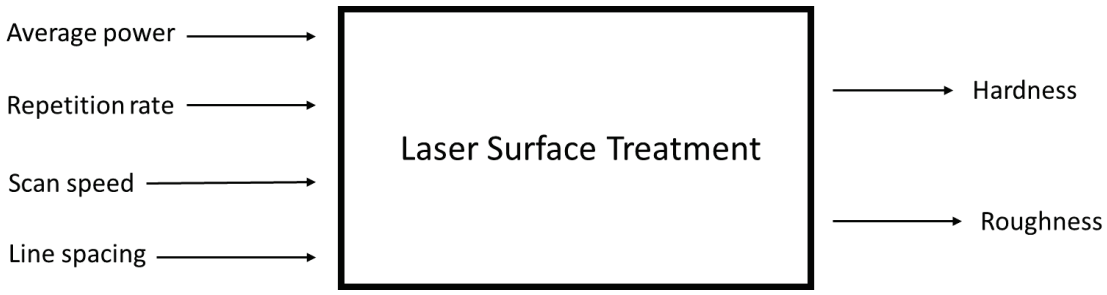

Figure 5.4. Black box of laser surface treatment

Table 5.3. Building information

File Version	**13.0.5.0**		
Study Type	Factorial	**Subtype**	Randomized
Design Type	Full Factorial	**Runs**	81.00
Design Model	2FI	**Blocks**	No Blocks
Center Points	0.0000	**Build Time (ms)**	1.0000

Table 5.4. 3^4 Full factorial DoE

		Factor 1	**Factor 2**	**Factor 3**	**Factor 4**
Std	Experimental Run	Average power (A)	Repetition rate (B)	Scan speed (C)	Line spacing (D)
		[W]	[kHz]	[mm/s]	[μm]
1	1	10	20	10	20
28	2	10	20	10	30
55	3	10	20	10	40
10	4	10	20	50	20
37	5	10	20	50	30
64	6	10	20	50	40
19	7	10	20	90	20
46	8	10	20	90	30
73	9	10	20	90	40
4	10	10	60	10	20
31	11	10	60	10	30

(cont. on next page)

Table 5.4 (cont.)

58	12	10	60	10	40
13	13	10	60	50	20
40	14	10	60	50	30
67	15	10	60	50	40
22	16	10	60	90	20
49	17	10	60	90	30
76	18	10	60	90	40
7	19	10	100	10	20
34	20	10	100	10	30
61	21	10	100	10	40
16	22	10	100	50	20
43	23	10	100	50	30
70	24	10	100	50	40
25	25	10	100	90	20
52	26	10	100	90	30
79	27	10	100	90	40
2	28	15	20	10	20
29	29	15	20	10	30
56	30	15	20	10	40
11	31	15	20	50	20
38	32	15	20	50	30
65	33	15	20	50	40
20	34	15	20	90	20
47	35	15	20	90	30
74	36	15	20	90	40
5	37	15	60	10	20
32	38	15	60	10	30
59	39	15	60	10	40
14	40	15	60	50	20
41	41	15	60	50	30
68	42	15	60	50	40
23	43	15	60	90	20
50	44	15	60	90	30
77	45	15	60	90	40
8	46	15	100	10	20
35	47	15	100	10	30
62	48	15	100	10	40
17	49	15	100	50	20
44	50	15	100	50	30
71	51	15	100	50	40
26	52	15	100	90	20
53	53	15	100	90	30
80	54	15	100	90	40
3	55	20	20	10	20
30	56	20	20	10	30
57	57	20	20	10	40
12	58	20	20	50	20
39	59	20	20	50	30
66	60	20	20	50	40

(cont. on next page)

Table 5.4 (cont.)

21	61	20	20	90	20
48	62	20	20	90	30
75	63	20	20	90	40
6	64	20	60	10	20
33	65	20	60	10	30
60	66	20	60	10	40
15	67	20	60	50	20
42	68	20	60	50	30
69	69	20	60	50	40
24	70	20	60	90	20
51	71	20	60	90	30
78	72	20	60	90	40
9	73	20	100	10	20
36	74	20	100	10	30
63	75	20	100	10	40
18	76	20	100	50	20
45	77	20	100	50	30
72	78	20	100	50	40
27	79	20	100	90	20
54	80	20	100	90	30
81	81	20	100	90	40

5.2.1. Laser Surface Treatment (LST)

For the laser surface treatment process, a commercially available industrial ytterbium low power pulsed fiber laser was used. The specification of fiber laser is given in Table 5.5.

The experimental setup is also given in Figure 5.5. As seen in Figure 5.5, a galvo scanner with a maximum scanning speed of 3000 $mm \cdot s^{-1}$ was used to control the movement of the laser beam and all the experiments were performed on the focal position. After laser treatment, the visual change on laser treated surface is shown in Figure 5.6

5.2.2. Measurement Techniques

Two measurement techniques were used to measure surface properties of tool steel. The first one is hardness and the second one is hardness measurements. All the measurement and experimental study was performed in LATARUM (Laser Technologies Research and Application Center) which is located in Kocaeli University Technopark.

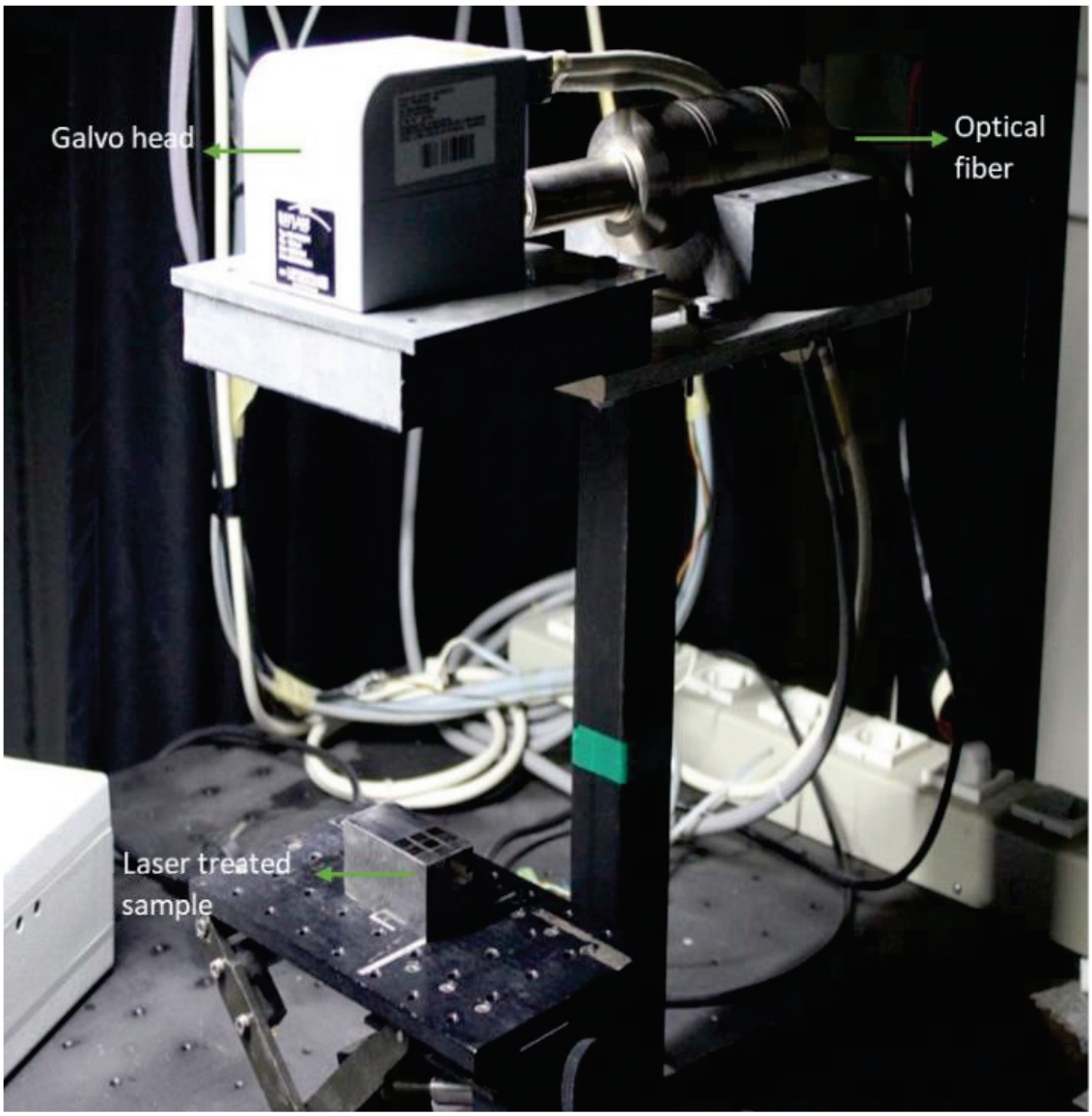

Figure 5.5. Laser surface treatment processing by using the fiber laser

In all measurements, a laser treated area measured three times from three different points and the average of these three measurements was taken as a result.

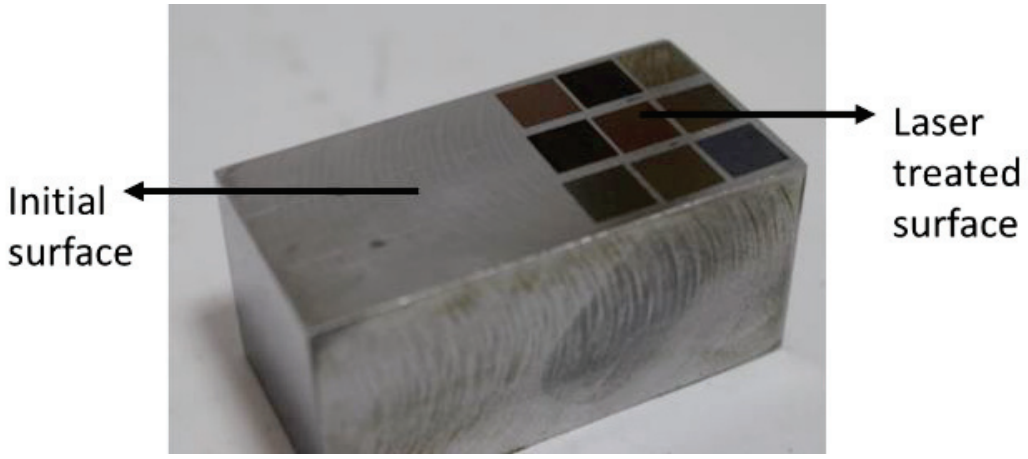

Figure 5.6. Laser treated surface of 1.2379 cold work tool steel

5.2.2.1. Hardness Measurement

The resistance of a substance to indentation is determined by hardness testing. Vickers hardness testing is one of the oldest methods of hardness testing, and it has a broad hardness scale that makes it ideal for most metals and welds. A 136° pyramidal diamond indenter with a square indent is used in the Vickers hardness test [89]. In this experiment (P=0.5 kg) load was applied for 8 seconds by reference to the ASTM E384 standard. The hardness (HV) is expressed by Equation 5.1. In Equation 5.1, F represents the applied load (measured in kilogram-force) and D^2 represents the area of indentation (measured in square millimeters). Vickers hardness measurement is shown in Figure 5.7.

$$HV = 1.854\ (F/D^2) \qquad \textbf{(5.1)}$$

5.2.2.2.Roughness Measurement

Surface roughness is a set of non-directional parameters that describes how smooth a surface texture is in regions smaller than three dimensions [90]. In the experiments, the roughness values of the surface were measured with a Time 3200 needle (stylus) tipped roughness measuring device as shown in Figure 5.8.

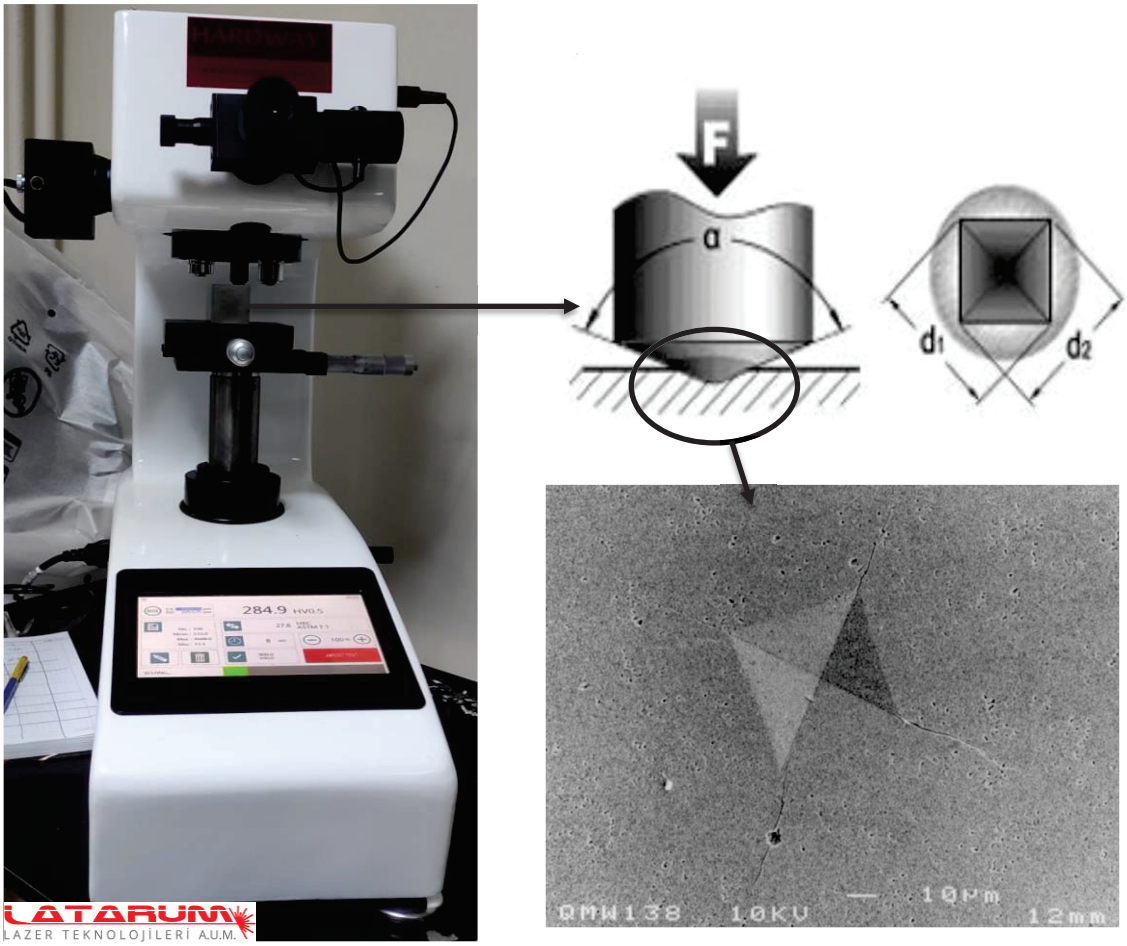

Figure 5.7. Vickers hardness measurement

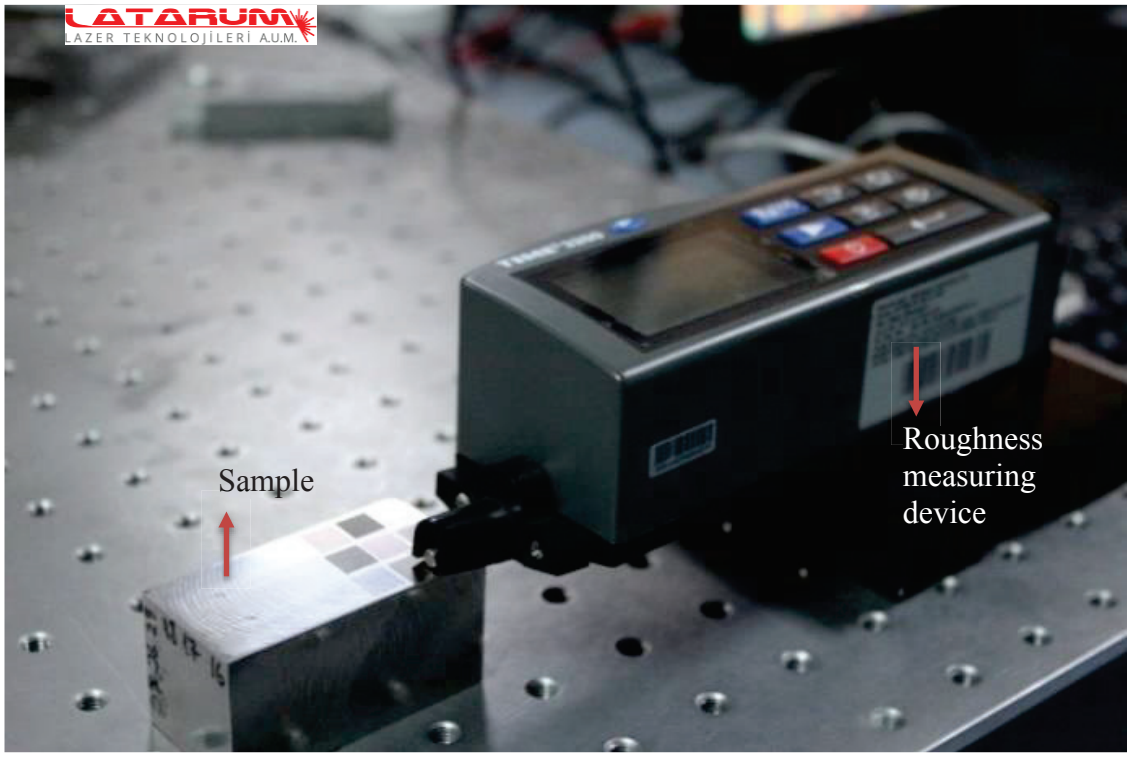

Figure 5.8. Roughness (Ra) measurement.

Table 5.5. Ytterbium low power pulsed fiber laser specifications [91]

Parameter	Value	Unit
Nominal average output power	20	W
Energy per pulse (at 20 kHz)	1	mJ
Pulse duration	<50	ns
Pulse peak power (at 20 kHz)	>20	kW
Pulse repetition rate	20 - 100	kHz
Laser wavelength	1080	nm

CHAPTER 6

RESULTS AND DISCUSSION

6.1. Problem Statement

Roughness and hardness are the main surface characteristics of cold work tool steels in the industry. These types of steels are used in die and mold industry so they need to be a specific hardness and roughness value to manufacture parts that has same surface properties and sometimes the surface properties of these mold can be change in the mass production for this reason they can be treated by laser to obtain specific surface properties.

Laser surface treatment is a useful method that changes the surface properties of materials. However, LST is a nonlinear process so numerical modeling is required to understand this process. In this thesis laser parameters optimization study was performed by using four different laser parameters as input and optimum hardness and roughness parameters are specified.

In the first part of this thesis an experimental study was performed on 1.2379 cold work tool steel. Firstly, the steel was treated with laser using different parameters then roughness and hardness were measured. Following that, twelve regression models were used to find the best fit using experimental data. At the end of the study minimum and maximum values of hardness and roughness were determined in the optimization process. Therefore, which parameters should be used to find minimum or maximum surface properties can be seen in this thesis. Moreover, by using regression equation and optimization methods predictions about laser input parameters can be performed according to required surface properties. Additionally, experimental results showed that LST is a very effective process to increase or decrease hardness and roughness of 1.2379 cold work tool steel.

6.2. Experimental Results

In this work, experiments were conducted to determine two primary surface characteristics: roughness and hardness.

6.2.1. Experimental Results for Hardness

After LST process hardness of 1.2379 cold work tool steel surface is measured and measurement results are presented in Table 6.1. Each of the 81 experimental runs was measured three times from various positions on the surface, and the average hardness is shown as given in Table 6.1. The experimental runs were all carried out with various laser input settings. 307 (HV0.5) is the initial hardness value of the material used in the experiment. The table demonstrates the hardness's change from its initial value. A laser can improve hardness to 80%, as seen experimental run 57. This improvement in hardness value shows that the laser has an effect on 1.2379 materials and is a suitable method for use in order to improve hardness in industry.

Table 6.1. Experimental results for hardness measurement

Experimental Run	**Hardness**			**Average Hardness**	**Change**
	Test 1	**Test 2**	**Test 3**		
	[HV0.5]	[HV0.5]	[HV0.5]	[HV0.5]	[%]
1	371	319	336	342.00	11.401
2	299	304	311	304.67	-0.760
3	293	304	315	304.00	-0.977
4	309	286	343	312.67	1.846
5	379	312	359	350.00	14.007
6	300	330	322	317.33	3.366
7	347	320	343	336.67	9.663
8	305	280	325	303.33	-1.194
9	318	305	295	306.00	-0.326
10	286	291	331	302.67	-1.412
11	373	323	326	340.67	10.966
12	328	302	325	318.33	3.692
13	292	302	305	299.67	-2.389
14	287	283	299	289.67	-5.646
15	302	306	331	313.00	1.954
16	415	377	343	378.33	23.236
17	369	326	334	343.00	11.726

(cont. on next page)

Table 6.1 (cont.)

18	292	337	324	317.67	3.474
19	388	346	390	374.67	22.041
20	328	344	320	330.67	7.709
21	354	389	390	377.67	23.018
22	320	363	324	335.67	9.338
23	337	299	323	319.67	4.126
24	317	304	325	315.33	2.714
25	292	298	324	304.67	-0.760
26	340	374	356	356.67	16.178
27	409	344	300	351.00	14.332
28	433	440	392	421.67	37.351
29	470	460	425	451.67	47.123
30	445	398	409	417.33	35.939
31	296	303	311	303.33	-1.194
32	398	395	418	403.67	31.488
33	350	335	382	355.67	15.852
34	345	360	359	354.67	15.527
35	402	384	385	390.33	27.144
36	394	376	422	397.33	29.425
37	445	420	424	429.67	39.957
38	402	427	443	424.00	38.111
39	469	436	428	444.33	44.734
40	388	354	355	365.67	19.110
41	386	416	410	404.00	31.596
42	402	405	390	399.00	29.967
43	350	322	352	341.33	11.183
44	392	386	376	384.67	25.299
45	382	368	365	371.67	21.064
46	444	432	465	447.00	45.603
47	371	373	423	389.00	26.710
48	520	473	459	484.00	57.655
49	447	423	413	427.67	39.305
50	379	411	399	396.33	29.099
51	439	430	417	428.67	39.631
52	395	396	402	397.67	29.533
53	448	418	420	428.67	39.631
54	464	423	414	433.67	41.260
55	555	519	501	525.00	71.010
56	467	506	502	491.67	60.152
57	571	555	525	550.33	79.262
58	382	421	374	392.33	27.796
59	378	370	383	377.00	22.801
60	435	374	391	400.00	30.293
61	355	354	372	360.33	17.372
62	322	400	415	379.00	23.453
63	406	401	422	409.67	33.442

(cont. on next page)

Table 6.1 (cont.)

64	452	486	508	482.00	57.003
65	423	450	471	448.00	45.928
66	505	500	473	492.67	60.478
67	410	393	432	411.67	34.093
68	403	408	385	398.67	29.859
69	371	408	400	393.00	28.013
70	394	396	377	389.00	26.710
71	375	372	354	367.00	19.544
72	346	371	430	382.33	24.539
73	403	408	392	401.00	30.619
74	515	506	474	498.33	62.324
75	494	430	480	468.00	52.443
76	457	400	478	445.00	44.951
77	416	378	392	395.33	28.773
78	392	412	401	401.67	30.836
79	344	383	347	358.00	16.612
80	346	333	380	353.00	14.984
81	369	348	354	357.00	16.287

6.2.2. Experimental Results for Roughness

The surface roughness properties of 1.2379 cold work tool steel are measured after LST process and measurement results are shown in Table 6.2. With various laser input parameters, 81 experimental runs were performed by using a low power fiber laser. The results of each experimental run were measured three times from various points on the surface, and the mean values were calculated as shown in Table 6.2. The material used in the experiment has an initial roughness of 0.485μm. The table also displays the roughness's change from the initial value. According to the results of experiments, laser surface treatment process on 1.2379 cold work tool steel can be reduced by up 33% (as seen experimental run 13); and also can be increased roughness by up to 243% (as seen experimental run 28). The experimented 1.2379 cold work tool steel has a low initial roughness compared to the other experimented tool steel. Since the materials used in this experiment (1.2379 cold work tool steel) are less initial roughness than the ones used in the literature, the experiments' roughness value could only be decreased by 33%. It has been shown that the roughness value may be decreased by employing a laser up to 0.323μm. This value provides evidence that the material used in the experiment can be quite smooth.

Table 6.2. Experimental results for roughness measurement

Experimental Run	Roughness			Avarage Roughness	Change
	Test 1	Test 2	Test 3		
	[μm]	[μm]	[μm]	[μm]	[%]
1	0.853	0.692	0.775	0.773	59.450
2	0.52	0.555	0.649	0.575	18.488
3	0.625	0.644	0.62	0.630	29.828
4	0.366	0.353	0.414	0.378	-22.131
5	0.554	0.535	0.403	0.497	2.543
6	0.399	0.401	0.369	0.390	-19.656
7	0.362	0.389	0.343	0.365	-24.811
8	0.421	0.54	0.484	0.482	-0.687
9	0.434	0.407	0.412	0.418	-13.883
10	0.622	0.593	0.605	0.607	25.086
11	0.533	0.541	0.522	0.532	9.691
12	0.629	0.635	0.629	0.631	30.103
13	0.300	0.318	0.357	0.325	-32.990
14	0.497	0.496	0.463	0.485	0.069
15	0.467	0.325	0.412	0.401	-17.251
16	0.37	0.347	0.34	0.352	-27.354
17	0.331	0.376	0.359	0.355	-26.735
18	0.292	0.389	0.287	0.323	-33.471
19	0.531	0.678	0.645	0.618	27.423
20	0.699	0.678	0.621	0.666	37.320
21	0.621	0.624	0.709	0.651	34.296
22	0.460	0.526	0.551	0.512	5.636
23	0.480	0.45	0.476	0.469	-3.368
24	0.513	0.511	0.573	0.532	9.759
25	0.621	0.583	0.582	0.595	22.749
26	0.372	0.391	0.354	0.372	-23.230
27	0.465	0.471	0.563	0.500	3.024
28	1.397	1.748	1.851	1.665	243.368
29	0.871	1.038	1.036	0.982	102.405
30	0.932	0.82	0.973	0.908	87.285
31	0.699	0.735	0.821	0.752	54.983
32	0.397	0.415	0.366	0.393	-19.038
33	0.532	0.520	0.425	0.492	1.512
34	0.408	0.339	0.329	0.359	-26.048
35	0.309	0.348	0.357	0.338	-30.309
36	0.339	0.46	0.395	0.398	-17.938
37	0.733	0.793	0.88	0.802	65.361
38	0.713	0.576	0.685	0.658	35.670
39	0.645	0.583	0.548	0.592	22.062
40	0.399	0.439	0.389	0.409	-15.670
41	0.333	0.438	0.418	0.396	-18.282
42	0.438	0.455	0.537	0.477	-1.718

(cont. on next page)

Table 6.2 (cont.)

43	0.439	0.433	0.437	0.436	-10.034
44	0.356	0.312	0.371	0.346	-28.591
45	0.346	0.442	0.45	0.413	-14.914
46	0.91	0.787	0.887	0.861	77.595
47	1.120	0.989	0.857	0.989	103.849
48	1.215	1.193	1.067	1.158	138.832
49	0.487	0.369	0.525	0.460	-5.086
50	0.438	0.432	0.361	0.410	-15.395
51	0.424	0.428	0.422	0.425	-12.440
52	0.54	0.58	0.501	0.540	11.409
53	0.57	0.586	0.586	0.581	19.725
54	0.474	0.484	0.456	0.471	-2.818
55	0.997	1.104	1.075	1.059	118.282
56	0.897	0.886	0.926	0.903	86.186
57	0.719	0.637	0.686	0.681	40.344
58	0.665	0.597	0.709	0.657	35.464
59	0.661	0.73	0.753	0.715	47.354
60	0.723	0.620	0.637	0.660	36.082
61	0.565	0.647	0.624	0.612	26.186
62	0.479	0.536	0.571	0.529	9.003
63	0.751	0.759	0.81	0.773	59.450
64	0.669	0.714	0.559	0.647	33.471
65	0.798	0.764	0.891	0.818	68.591
66	0.814	0.856	0.911	0.860	77.388
67	0.730	0.712	0.611	0.684	41.100
68	0.565	0.472	0.512	0.516	6.460
69	0.700	0.709	0.645	0.685	41.168
70	0.591	0.634	0.725	0.650	34.021
71	0.651	0.547	0.601	0.600	23.643
72	0.697	0.583	0.728	0.669	38.007
73	1.087	1.135	1.14	1.121	131.065
74	1.327	1.386	1.14	1.284	164.811
75	1.418	1.26	1.422	1.367	181.787
76	0.435	0.522	0.564	0.507	4.536
77	0.607	0.538	0.552	0.566	16.632
78	0.662	0.551	0.65	0.621	28.041
79	0.580	0.619	0.68	0.626	29.141
80	0.586	0.542	0.596	0.575	18.488
81	0.567	0.687	0.695	0.650	33.952

6.3. Neuro-Regression Modelling Results

Regression analysis is one of the primary techniques for estimating parameters, verifying and testing the model's accuracy. In this thesis, neuro regression analysis was used. In order to obtain the best results in optimization, 12 different mathematical models were tested. Table 6.3 includes a list of the mathematical models' names and formulas used in modeling study. In the mathematical modelling, the data collected from the experiments was separated into three groups randomly: 80% training data, 20% testing data, and 10% validation data that is selected from training data as shown in Appendix A.

Regression analyses were carried out by using Wolfram Mathematica 11.3. The aim of this part is to develop a mathematical model and use these models to obtain the best R^2 values. In Wolfram Mathematica tool, four laser parameters ((i.e., power, frequency, scan speed and line spacing) were used as input data and R^2 training, R^2 training adjusted, R^2 testing, R^2 validation, maximum and minimum values of the models were calculated for hardness and roughness.

Table 6.4 presents the neuro regression results of 12 different regression models for hardness. In model selection, the first step is to check R^2 training value. R^2 training value is expected to be greater than 0.95, and close enough to 1. R^2 training value of SONTNR is lower than 0.95 thus it is not a suitable model. R^2 training adjusted also should be greater than 0.95, and close enough to 1, so SONTN is not a suitable model. R^2 testing and R^2 Validation values expected to be greater than 0.7 and close enough to 1. Additionally, we need to check maximum and minimum values, these values should be in the range of experimental study results if these values are so high or lower than experimented results it means that the model is not suitable. In model FOLN, FOLNR, FOTN, FOTNR, L, LR, and SOLNR R^2 testing or R^2 Validation is lower than 0.7. In model SONR and FOTNR maximum or minimum value is quite different than experimental results. Model SOLN is suitable, but model SON has better results than SOLN. When we look at these arguments the best model is Second Order Multiple Non-Linear (SON) for hardness. The regression equation for hardness is given by Equation 6.1. and Wolfram Mathematica 11.3 code is given in Appendix B

Table 6.3. Regression models (linear, quadratic, trigonometric, logarithmic, and their rational forms)

Model Name	Nomenclature	Formula
Multiple linear	L	$Y = \sum_{i=1}^{2}(a_i x_i) + c$
Multiple linear rational	LR	$Y = \frac{\sum_{i=1}^{2}(a_i x_i) + c_1}{\sum_{j=1}^{2}(\beta_j x_j)} + c_2$
Second order multiple non-linear	SON	$Y = \sum_{k=1}^{2}\sum_{j=1}^{2}(a_j x_j x_k) + \sum_{i=1}^{2}(a_i x_i) + \ c$
Second order multiple non-linear rational	SONR	$Y = \frac{\sum_{k=1}^{2}\sum_{j=1}^{2}(a_j x_j x_k) + \sum_{i=1}^{2}(a_i x_i) + \ c_1}{\sum_{l=1}^{2}\sum_{m=1}^{2}(\beta_m x_m x_l) + \sum_{n=1}^{2}(\beta_n x_n)} + c_2$
First order trigonometric multiple non-linear	FOTN	$Y = \sum_{i=1}^{2}(a_i Sin[x_i] + a_i Cos[x_i]) + c$
First order trigonometric multiple non-linear rational	FOTNR	$Y = \frac{\sum_{i=1}^{2}(a_i Sin[x_i] + a_i Cos[x_i]) + c_1}{\sum_{j=1}^{2}(\beta_j Sin[x_j] + \gamma_j Cos[x_j])} + c_2$
Second order trigonometric multiple non-linear	SOTN	$Y = \sum_{i=1}^{2}(a_i Sin[x_i] + a_i Cos[x_i]) + \sum_{j=1}^{2}(\beta_j Sin^2[x_j] + \gamma_j Cos^2[x_j]) + c$
Second order trigonometric multiple non-linear rational	SOTNR	$Y = \frac{\sum_{i=1}^{2}(a_i Sin[x_i] + a_i Cos[x_i]) + \sum_{j=1}^{2}(\beta_j Sin^2[x_j] + \gamma_j Cos^2[x_j]) +}{\sum_{k=1}^{2}(\theta_i Sin[x_k] + \theta_i Cos[x_k]) + \sum_{l=1}^{2}(\delta_j Sin^2[x_l] + \delta_j Cos^2[x_l])} + c_2$
First order logarithmic multiple non-linear	FOLN	$Y = \sum_{i=1}^{2}(a_i Log[x_i]) + c$
First order logarithmic multiple non-linear rational	FOLNR	$Y = \frac{\sum_{i=1}^{2}(a_i Log[x_i]) + c_1}{\sum_{j=1}^{2}(\beta_j Log[x_j])} + c_2$
Second order logarithmic multiple non-linear	SOLN	$Y = \sum_{k=1}^{2}\sum_{j=1}^{2}(a_j Log[x_j x_k]) + \sum_{i=1}^{2}(a_i Log[x_i]) + c$
Second order logarithmic multiple non-linear rational	SOLNR	$Y = \frac{\sum_{k=1}^{2}\sum_{j=1}^{2}(a_j Log[x_j x_k]) + \sum_{i=1}^{2}(a_i Log[x_i]) + c_1}{\sum_{m=1}^{2}\sum_{l=1}^{2}(a_l Log[x_l x_m]) + \sum_{n=1}^{2}(a_n Log[x_n])} + c_2$

$$Hardness = -48.423171404381456 + 53.7463982105139 66A - 1.2895367785586829A^2 + 0.2894129750949088B - 0.051099066861209 86AB + 0.0034789141909866 49B^2 + 0.23508834667309295C - 0.13799804738829238AC + 0.0032076905247195977BC + 0.009906130971054996C^2 - 2.5804182412177843D + 0.11377801148037163AD - 0.0000332097260537434 2BD + 0.0015986507618359755CD + 0.020561419127851806D^2 \quad \textbf{(6.1)}$$

Table 6.4. Neuro-regression results for Hardness

Models	R^2 Training	R^2 Training Adjusted	R^2 Testing	R^2 Validation	Maximum	Minimum
FOLN	0.992382	0.990997	0.683378	0.479235	457.311	308.744
FOLNR	0.995409	0.994574	0.764166	0.627922	526.721	292.51
FOTN	0.993483	0.990987	0.697218	0.689192	459.022	245.913
FOTNR	0.997073	0.995952	0.570459	0.793735	383.213	-1.41651E+14
L	0.991364	0.989794	0.629856	0.43403	453.725	311.687
LR	0.995251	0.994388	0.751477	0.610908	521.129	290.374
SOLN	0.995876	0.992341	0.809924	0.722725	476.021	310.424
SOLNR	0.998086	0.996445	0.569544	0.85709	551.691	290.011
SON	0.996052	0.992668	0.803777	0.745642	495.131	305.14
SONR	0.998336	0.996909	0.721331	0.796014	2.46514*10^11	-7.54136*10^11
SONTN	0.997164	1.00737	0.745706	0.821036	538.388	171.056
SONTNR	0.19254	3.0994	-29.0528	-56.8289	6.64659*10^13	-7.24862*10^8

The neuro regression results for 12 different regression models for roughness are provided in Table 6.5. R^2 training for the models FOLN, L, and SONTNR is less than 0.95. Model FOLNR, FOTNR, LR, SOLNR, SONR, and SONTN do not match experimental data in terms of their maximum or lowest values. FOTNR, SOLN, and SON are appropriate roughness models, but SOLN is the best model since it has a higher R^2 value and maximum and minimum values are the most similar to experimental data. So, second order logarithmic multiple non-linear (SOLN) was chosen as a regression model for roughness. The roughness regression equation is given by Equation 6.2.

$$Roughness = 13.101401369628958 - 0.6017149469534143\text{Log}[A] + 0.224076548965367\text{Log}[A]^2 - 2.197884204350617\text{Log}[B] - 0.026019674360441367\text{Log}[A]\text{Log}[B] + 0.2034392270308284\text{Log}[B]^2 - 0.9750349690897032\text{Log}[C] - 0.12038213038747095\text{Log}[A]\text{Log}[C] + 0.026352255795680922\text{Log}[B]\text{Log}[C] + 0.09202525848454077\text{Log}[C]^2 - 3.6569776646819023\text{Log}[D] + 0.08270606484083204\text{Log}[A]\text{Log}[D] + 0.18517796804950598\text{Log}[B]\text{Log}[D] + 0.12217230592057576\text{Log}[C]\text{Log}[D] + 0\ 0.33601719919784856\text{Log}[D]^2 \quad (\mathbf{6.2})$$

Table 6.5. Neuro-regression results for Roughness

Models	R^2 Training	R^2 Training Adjusted	R^2 Testing	R^2 Validation	Maximum	Minimum
FOLN	0.938542	0.927368	0.714816	0.423023	0.947295	0.314558
FOLNR	0.964655	0.958228	0.581109	0.631264	3.75357*10^6	-1.25074E+11
FOTN	0.950077	0.930958	0.746978	0.783079	1.05745	0.118529
FOTNR	0.983791	0.977584	0.5683	0.761073	5.62508*10^10	-3.64579*10^13
L	0.927747	0.91461	0.673494	0.287902	0.900524	0.314653
LR	0.963459	0.956815	0.585858	0.583591	[Infinity]	-\[Infinity]
SOLN	0.957106	0.920339	0.717587	0.810759	1.0153	0.277508
SOLNR	0.993495	0.987919	-0.71429	0.963465	0.629621	-1.23858*10^12
SON	0.955194	0.916788	0.72336	0.798226	1.02841	0.250542
SONR	0.993904	0.988679	-42.1369	0.962665	1.88338*10^13	-1.77502E+12
SONTN	0.973767	1.06821	0.766541	0.786259	1.63377	0.0387422
SONTNR	0.647455	1.91662	-1.67265	-1.36577	2.13247	-8509560000

6.4. Optimization Results

The final material characteristics can be precisely controlled by selecting the proper laser parameters. This allows processing techniques to be designed and improved to offer the optimal material functioning for its expected performance [30].

The purpose of this section of the thesis is to minimize and maximize roughness and hardness of 1.2379 cold work tool steel and specify the input parameters of laser device required for this process. Surface roughness and hardness of 1.2379cold work tool steel was optimized by using two scenarios for each output. It is aimed to find minimum

and maximum values of given outputs to see the effect of laser on surface properties. As mentioned in Chapter 4, there are two main optimization techniques which are traditional and non-traditional. In this thesis non-traditional, in other word stochastic optimization methods were used. To investigate different optimization algorithms and compare them, “Differential Evolution”, “Simulated Annealing”, “Random Search” and “Nelder-Mead” algorithms were performed on "Wolfram MATHEMATICA 11.3" with the help of “NMinimize” and “NMaximize” tool. These tools maximize and minimize objective function and give us optimum input parameters for required solution. Optimization scenarios for hardness and roughness are given in Table 6.6. The best equations selected for hardness (Equation 6.1) and roughness (Equation 6.2) were used in the optimization study. The code written for hardness optimization is given in Appendix C.

For the experimented range of laser parameters, in scenario 1 minimum hardness, in scenario 2 maximum hardness, in scenario 3 minimum roughness and in scenario 4 maximum hardness was evaluated.

Table 6.6. Optimization scenarios for each problem (A:Average power, B:Repetition rate, C:Scan speed, D:Line spacing)

Scenario	Optimization Problem 1 (Hardness)	Scenario	Optimization Problem 2 (Roughness)
1	$10 \leq A \leq 20$ $20 \leq B \leq 100$ $10 \leq C \leq 90$ $20 \leq D \leq 40$	3	$10 \leq A \leq 20$ $20 \leq B \leq 100$ $10 \leq C \leq 90$ $20 \leq D \leq 40$
2	$10 \leq A \leq 20$ $20 \leq B \leq 100$ $10 \leq C \leq 90$ $20 \leq D \leq 40$	4	$10 \leq A \leq 20$ $20 \leq B \leq 100$ $10 \leq C \leq 90$ $20 \leq D \leq 40$

6.4.1. Optimization Results for Hardness

Table 6.7 gives the results of the 1.2379 material's surface hardness optimization In the table 6.7 objective function is surface hardness. All optimization algorithms (MNM, MDE, MSA, MRS) produced the same output values and laser input parameters. The minimum hardness value was found to be 305(HV0.5) in scenario 1. This value is almost the same as the initial hardness value. But although the minimum hardness

optimization did not change the hardness, the roughness value decreased by 21% to 0.381 μm. These output values can be reached by applying laser parameters as: average power=10W repetition rate=20kHz Scan speed=51.879mm/s and D=33.080 μm.

In scenario 2, maximum hardness was investigated. Results of optimization showed that optimization algorithm gave the same outcomes. Hardness value increase from 307(HV0.5) to 495(HV0.5), it means that hardness value can be increased 61% by applying laser on the surface. While hardness value increases, roughness value also increases to 0.99 μm. These surface properties can be reach by applying laser parameters as average power=20W, repetition rate=20kHz, scan speed=10mm/s and D=40 μm

6.4.2. Optimization Results for Roughness

Table 6.7 displays the outcomes of the surface roughness optimization for the 1.2379 material. Surface roughness is the objective function in Table 6.7. Exactly the same output values and laser input parameters were obtained by all optimization methods (MNM, MDE, MSA, and MRS). In scenario 3, minimum roughness was evaluated as 0277 μm. It is observed that the optimized minimum roughness value is 43% lower than the initial value. While minimize the roughness value hardness value almost never changed. Thus, it is possible to reduce roughness without any change in hardness value. For optimum minimum roughness value laser parameters should be entered as follows: average power=10W, repetition rate=42.221kHz, scan speed=55.284mm/s and D=29.888 μm.

In scenario 4 maximum roughness value was evaluated as 1.219 μm and the value of hardness is 476 (HV.05). For this scenario laser input parameters should be as follows: average power=20W, repetition rate=20kHz, scan speed=10mm/s and D=20 μm.

Convergence graphics of maximum hardness and minimum roughness for MNM, MDE, MSA, MRS optimization algorithms are given in Figure 6.1 and Figure 6.2, respectively. The figures show that after how many iterations the optimization algorithms approach the optimum value. Even if the number of iterations is completely different for each algorithm, all optimization algorithms employed in this study achieved the same results. The optimum value was found after about 30 iterations for MNM and MDE algorithms for both objective functions. Although the optimum value was found for the MSA algorithm after about 80 iterations, different values continued to be tested, but it

still coming back to the same value. While the MRS method provides a linear response for maximum hardness, for the minimum roughness value algorithm starts at the optimum and returns to the same value after checking different points.

Table 6.7. Results of the optimization problem for Hardness

Scenario No	Constraints	Optimization Algorithms	Output1 Hardness (HV0.5)	Output2 Roughness (µm)	Suggested Design
1	$10 \le A \le 20$ $20 \le B \le 100$ $10 \le C \le 90$ $20 \le D \le 40$	MNM	305.1403626832	0.38134832257247	A=10, B=20, C=51.879, D= 33.08051
		MDE	305.1403627017	0.38134749177500	A=10, B=20, C=51.881, D=33.0807
		MSA	305.1403631509	0.38134832257247	A=10, B=20, C=51.8797, D=33.0805
		MRS	305.1403631977	0.38134832257247	A=10, B=20, C=51.8797, D=33.0805
2	$10 \le A \le 20$ $20 \le B \le 100$ $10 \le C \le 90$ $20 \le D \le 40$	MNM	495.1305476713	0.99234004218314	A=20, B=20, C=10, D=40
		MDE	495.1305475844	0.99234004218314	A=20, B=20, C=10, D=40
		MSA	495.1305475844	0.99234004218314	A=20, B=20, C=10, D=40
		MRS	495.1305476713	0.99234004218314	A=20, B=20, C=10, D=40

Table 6.8. Results of the optimization problem for Roughness

Scenario No	Constraints	Optimization Algorithms	Output1 Hardness (HV0.5)	Output2 Roghness (µm)	Suggested Design
3	$10 \le A \le 20$ $20 \le B \le 100$ $10 \le C \le 90$ $20 \le D \le 40$	MNM	309.25234746203	0.2775083130330	A=10, B=42.2215743 C=55.284 D= 29.8886
		MDE	309.25234746203	0.2775083126674	A=10, B=42.2215743 C=55.284 D= 29.8886
		MSA	309.25234746203	0.2775083130310	A=10, B=42.2215743 C=55.284 D= 29.8886
		MRS	309.25234746203	0.2775083130310	A=10, B=42.2215743 C=55.284 D= 29.8886
4	$10 \le A \le 20$ $20 \le B \le 100$ $10 \le C \le 90$ $20 \le D \le 40$	MNM	476.24755868823	1.2190076134084	A=20, B=20, C=10, D=20
		MDE	476.24755868823	1.2190076134084	A=20, B=20, C=10, D=20
		MSA	476.24755868823	1.2190076125101	A=20, B=20, C=10, D=20
		MRS	476.24755868823	1.2190076134084	A=20, B=20, C=10, D=20

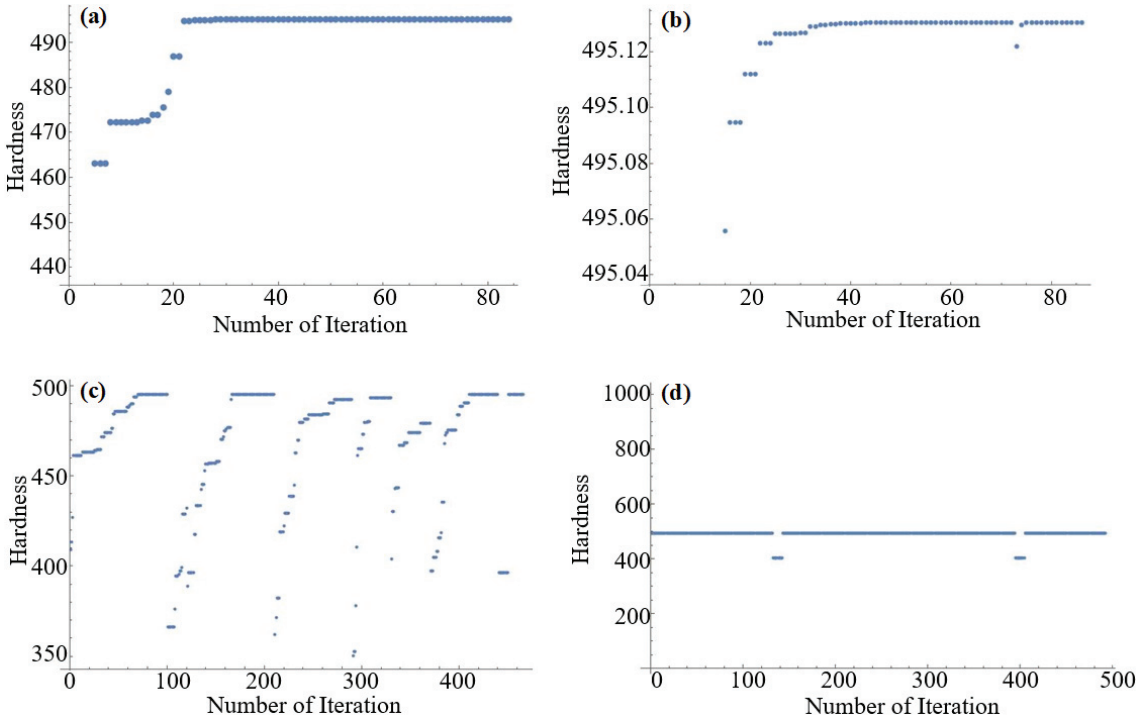

Figure 6.1. Convergence graphics of stochastic algorithms for maximum hardness
a) MNM, b) MDE, c) MSA, d) MRS

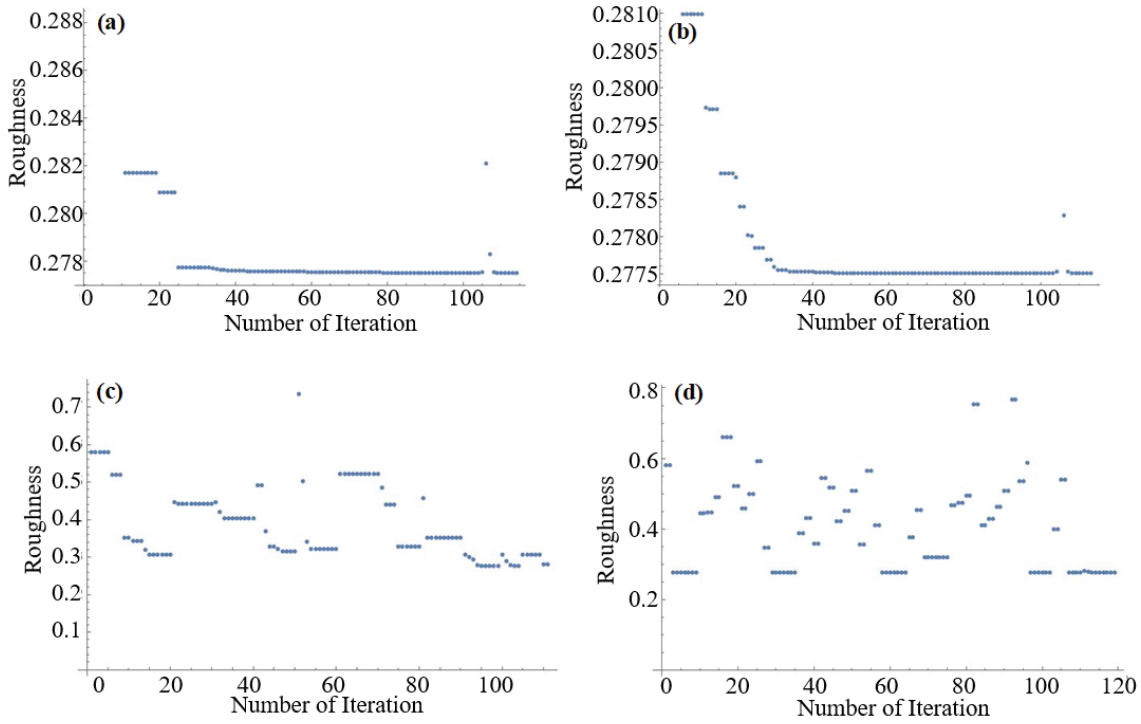

Figure 6.2. Convergence graphics of stochastic algorithms for minimum roughness
a) MNM, b) MDE, c) MSA, d) MRS

CHAPTER 7

CONCLUSION

In this thesis, a laser surface treatment optimization study was performed by using a commercially available low-power fiber laser. The research includes experimental studies, regression analysis, and optimization studies. Experimental studies were performed on 1.2379 cold work tool steel which is a widely used tool steel in industry. Laser parameters such as average power, repetition rate, line spacing and scan speed were specified as input parameters. The surface properties of the material (hardness and roughness) were measured after LST process and these surface properties were used as output parameters. Input parameters were determined with 3^4 full factorial designs, and 81 experimental runs were created by using Design-Expert software. Each experimented surface parameter resulting in 81 experimental runs were measured three times to obtain mean values. Hence, 243 measurements for hardness and 243 measurements for roughness were used as output. As the next step of the thesis, regression analysis using twelve different models was established for each output by using Wolfram MATHEMATICA 11.3. Thus, by trying different regression models, the model with the best/highest R^2 values to be used in the optimization study could be selected. As a result of regression analysis, it is obtained that the second order multiple non-linear model is the best regression equation for hardness and the second order logarithmic multiple non-linear model is the best for roughness. In the last part of this thesis, optimization study was performed by using non-traditional optimization techniques which are Differential Evolution, Simulated Annealing, Random Search and Nelder-Mead. Optimization study was applied using Wolfram MATHEMATICA 11.3. When different optimization algorithm results were compared, it can be depicted that all optimization algorithms gave almost the same results for both objective functions. Furthermore, optimization studies have shown that the hardness or roughness of 1.2379 cold-work steel can be increased or decreased by applying appropriate laser parameters.

In summary, this study showed that the surface properties of 1.2379 cold-work steel can be improved in a short period of time using a low-power fiber laser. Also, the laser parameters used in this study have a significant impact on the hardness and roughness properties of the material. Therefore, the laser parameters must be specified

precisely to obtain the desired surface properties. This study provides the possibility of specifying laser input parameters for expected roughness and hardness values using regression equations and optimization techniques. Only a few studies regarding LST of 1.2379 cold work tool steel have been published in the literature. This thesis study is the first study that uses a low power fiber laser to enhance the surface characteristics of this steel. Additionally, different from the previous studies, many regression models and optimization methods were employed in this thesis to optimize the hardness and roughness of 1.2379 cold work tool steel.

REFERENCES

(1) A. Montealegre, M.; Castro, G.; Rey, P.; Arias, J. L.; Vázquez, P.; González, M. Surface Treatments by Laser Technology. *Contemp. Mater.* **2010**, *1* (1), 19–30. https://doi.org/10.5767/anurs.cmat.100101.en.019M.

(2) Shukla, P.; Lawrence, J. Characterization and Modification of Technical Ceramics through Laser Surface Engineering. In *Laser Surface Engineering*; Elsevier, 2015; pp 107–134. https://doi.org/10.1016/B978-1-78242-074-3.00005-2.

(3) Steen, W. M. *Laser Material Processing*; Springer London: London, 1991. https://doi.org/10.1007/978-1-4471-3820-4.

(4) Tamanna, N.; Crouch, R.; Naher, S. Progress in Numerical Simulation of the Laser Cladding Process. *Opt. Lasers Eng.* **2019**, *122* (May), 151–163. https://doi.org/10.1016/j.optlaseng.2019.05.026.

(5) Vijay Arasu, I.; Chockalingam, K.; Kailasanathan, C.; Sivabharathy, M. Optimization of Surface Roughness in Selective Laser Sintered Stainless Steel Parts. *Int. J. ChemTech Res.* **2014**, *6* (5), 2993–2999.

(6) Matras, A. Research and Optimization of Surface Roughness in Milling of SLM Semi-Finished Parts Manufactured by Using the Different Laser Scanning Speed. *Materials (Basel).* **2019**, *13* (1), 9. https://doi.org/10.3390/ma13010009.

(7) Canel, T.; Zeren, M.; Sınmazçelik, T. Laser Parameters Optimization of Surface Treating of Al 6082-T6 with Taguchi Method. *Opt. Laser Technol.* **2019**, *120* (August), 105714. https://doi.org/10.1016/j.optlastec.2019.105714.

(8) Lesyk, D.; Dzhemelinskyi, V.; Martinez, S.; Lamikiz, A.; Danyleiko, O.; Hyzhevskyi, V. Laser Transformation Hardening Effect on Hardening Zone Features and Surface Hardness of Tool Steel AISI D2. *Mech. Adv. Technol.* **2017**, *1* (79), 26–33. https://doi.org/10.20535/2521-1943.2017.79.95851.

(9) Ukar, E.; Lamikiz, A.; López de Lacalle, L. N.; del Pozo, D.; Arana, J. L. Laser Polishing of Tool Steel with CO2 Laser and High-Power Diode Laser. *Int. J. Mach. Tools Manuf.* **2010**, *50* (1), 115–125. https://doi.org/10.1016/j.ijmachtools.2009.09.003.

(10) Ukar, E.; Lamikiz, A.; López De Lacalle, L. N.; Liebana, F.; Etayo, J. M. Laser Polishing Parameter Optimization for Die and Moulds Surface Finishing. *Proc. ASME Int. Manuf. Sci. Eng. Conf. MSEC2008* **2009**, *1* (January 2022), 197–204. https://doi.org/10.1115/MSEC_ICMP2008-72258.

(11) Ukar, E.; Lamikiz, A.; Martínez, S.; Tabernero, I.; Lacalle, L. N. L. De. Roughness Prediction on Laser Polished Surfaces. *J. Mater. Process. Technol.* **2012**, *212* (6), 1305–1313. https://doi.org/10.1016/j.jmatprotec.2012.01.007.

(12) Temmler, A.; Cortina, M.; Ross, I.; Küpper, M. E.; Rittinghaus, S.-K. Laser Micro Polishing of Tool Steel 1.2379 (AISI D2): Influence of Intensity Distribution, Laser Beam Size, and Fluence on Surface Roughness and Area Rate. *Metals (Basel)*. **2021**, *11* (9), 1445. https://doi.org/10.3390/met11091445.

(13) Akman, E. Femtosaniye Lazerle Metalik Nanoyapılarin Oluşturulması ve Biyolojik Uygulamaları, 2012.

(14) Luke, A. M.; Mathew, S.; Altawash, M. M.; Madan, B. M. Lasers: A Review with Their Applications in Oral Medicine. *J. Lasers Med. Sci.* **2019**, *10* (4), 324–329. https://doi.org/10.15171/jlms.2019.52.

(15) Williams, D. Laser Basics. *Anaesth. Intensive Care Med.* **2008**, *9* (12), 550–552. https://doi.org/10.1016/j.mpaic.2008.09.008.

(16) Quimby, R. S. *Photonics and Lasers*; Wiley, 2006.https://doi.org/10.1002/0471791598.

(17) Anık, S.; Öğür, A.; Vural, M. Termik Kesme Teknolojisi. **1996**.

(18) Jules Janick, James N. Cummins, Susan K. Brown, and M. H. T. The Laser Guidebook. *An Autom. Irrig. Syst. Using Arduino Microcontroller* **2011**, *1908* (January), 2–6.

(19) Selen, A. E. Investigation of the Microstructural and Mechanical Properties of DP600 and TRIP800 Steels Welded by Fiber Laser, 2021.

(20) Csele, M. *Fundamentals of Light Sources and Lasers*; John Wiley & Sons, Inc, 2004. https://doi.org/https://doi.org/10.1002/0471675210.

(21) Koechner, W.; Bass, M. *Solid-State Lasers*; Springer New York, 2003.

(22) Lim, H.; Ilday, F. Ö.; Wise, F. W. Generation of 2-NJ Pulses from a Femtosecond Ytterbium Fiber Laser. *Opt. Lett.* **2003**, *28* (8), 660. https://doi.org/10.1364/OL.28.000660.

(23) Aydın, Y. O. Development of a 60 W Pulsed Fiber Laser Amplifier for Materials Processing, 2014.

(24) Tavkaya, E. Vision-Based Monitoring and Control of Fiber Laser Welding, 2014.

(25) Weber, M. J. *Handbook of Lasers*; CRC Press, 2001. https://doi.org/10.1201/9781420050172.

(26) Chow, W. W.; Koch, S. W. Semiconductor-Laser Fundamentals: Physics of the Gain Materials. Springer-Verlag: Berlin-Germany 1999.

(27) Çalıgülü, U. The Investigation of Joinability Characteristics in the Laser Welding Method Couples of AISI 304-430 Stainless-AISI 1010 Steel, 2009.

(28) Karaağaçlı, A. Effect of Lazer Welding Parameters on Microstructure and Mechanical Properties in Automotive Applications, 2019.

(29) Sugioka, K.; Meunier, M.; Piqué, A. *Laser Precision Microfabrication*; Springer Series in Materials Science; Springer Berlin Heidelberg, 2010.

(30) Sugioka, K.; Michael, M.; Pique, A. *Laser Precise Microfabrication*; 2010.

(31) Gregson, V.; Bass, M. Laser Material Processing. *Holl. Holl. Publ. Co.* **1984**.

(32) Zhang, D.; Lei, T. C.; Zhang, J.; Ouyang, J. The Effects of Heat Treatment on Microstructure and Erosion Properties of Laser Surface-Clad Ni-Base Alloy. *Surf. Coatings Technol.* **1999**, *115* (2–3), 176–183. https://doi.org/10.1016/S0257-8972(99)00176-0.

(33) Hick, A. J. Rapid Surface Heat Treatments-a Review of Laser and Electron Beam Hardening. *Heat Treat. Met.* **1983**, *10* (1), 3–11.

(34) Yao, J. H.; Zhang, Q. L.; Kong, F. Z. Laser Remanufacturing to Improve the Erosion and Corrosion Resistance of Metal Components. In *Laser Surface Modification of Alloys for Corrosion and Erosion Resistance*; Elsevier, 2012; pp 320–354. https://doi.org/10.1533/9780857095831.2.320.

(35) Rottwinkel, B.; Nölke, C.; Kaierle, S.; Wesling, V. Laser Cladding for Crack Repair of CMSX-4 Single-Crystalline Turbine Parts. *Lasers Manuf. Mater. Process.* **2017**, *4* (1), 13–23. https://doi.org/10.1007/s40516-016-0033-8.

(36) Bartkowski, D.; Bartkowska, A. Wear Resistance in the Soil of Stellite-6/WC Coatings Produced Using Laser Cladding Method. *Int. J. Refract. Met. Hard Mater.* **2017**, *64*, 20–26. https://doi.org/10.1016/j.ijrmhm.2016.12.013.

(37) Zarini, S.; Previtali, B.; Vedani, M.; Rovatti, L. Cracks Susceptibility Elimination in Fiber Laser Cladding of Ni-Based Alloy With Addition of Tungsten Carbides. In *Volume 3: Engineering Systems; Heat Transfer and Thermal Engineering; Materials and Tribology; Mechatronics; Robotics*; American Society of Mechanical Engineers, 2014. https://doi.org/10.1115/ESDA2014-20623.

(38) Paul, S.; Thool, K.; Singh, R.; Samajdar, I.; Yan, W. Experimental Characterization of Clad Microstructure and Its Correlation with Residual Stresses. *Procedia Manuf.* **2017**, *10*, 804–818. https://doi.org/10.1016/j.promfg.2017.07.081.

(39) Zhu, Y.; Yang, Y.; Mu, X.; Wang, W.; Yao, Z.; Yang, H. Study on Wear and RCF Performance of Repaired Damage Railway Wheels: Assessing Laser Cladding to Repair Local Defects on Wheels. *Wear* **2019**, *430–431*, 126–136. https://doi.org/10.1016/j.wear.2019.04.028.

(40) Chakraborty, R.; Raza, M. S.; Datta, S.; Saha, P. Synthesis and Characterization of Nickel Free Titanium–Hydroxyapatite Composite Coating over Nitinol Surface through in-Situ Laser Cladding and Alloying. *Surf. Coatings Technol.* **2019**, *358*, 539–550. https://doi.org/10.1016/j.surfcoat.2018.11.036.

(41) K.R., R.; Bontha, S.; M.R., R.; Das, M.; Balla, V. K. Laser Surface Melting of Mg-Zn-Dy Alloy for Better Wettability and Corrosion Resistance for Biodegradable Implant Applications. *Appl. Surf. Sci.* **2019**, *480*, 70–82. https://doi.org/10.1016/j.apsusc.2019.02.167.

(42) Lu, Y.; Yang, C.; Liu, Y.; Yang, K.; Lin, J. Characterization of Lattice Defects and Tensile Deformation of Biomedical Co29Cr9W3Cu Alloy Produced by Selective Laser Melting. *Addit. Manuf.* **2019**, *30*, 100908. https://doi.org/10.1016/j.addma.2019.100908.

(43) Nyoni, E.; Akinlabi, E. T. Process Parameter Interaction Effect on the Evolving Properties of Laser Metal Deposited Titanium for Biomedical Applications. *Thin Solid Films* **2016**, *620*, 94–102. https://doi.org/10.1016/j.tsf.2016.09.060.

(44) Antoy, J. *Design of Experiments for Engineers and Scientists*; Elsevier, 2014. https://doi.org/10.1016/C2012-0-03558-2.

(45) Atalan, Y. A. In Pure and Applied Sciences Developing Optimization Models for Wind Energy Using Design of Experiment. **2020**, No. November.

(46) Montgomery, D.; Runger, G.; Hubele, N. *Engineering Statistics*; 1998.

(47) Aydin, L.; Artem, H. S.; Oterkus, S. Designing Engineering Structures Using Stochastic Optimization Methods. *Des. Eng. Struct. Using Stoch. Optim. Methods* **2020**. https://doi.org/10.1201/9780429289576.

(48) Cavazzuti, M. *Optimization Methods*; Springer Berlin Heidelberg: Berlin, Heidelberg, 2013; Vol. 53. https://doi.org/10.1007/978-3-642-31187-1.

(49) Vecchio, R. Del. *Understanding Design of Experiments*; USA, 1997; Vol. 35.

(50) Kutubi, H. S. AL. On Randomized Complete Block Design. *Int. J. Sci.* **2022**, No. April 2021.

(51) Tasgetiren, S. Kalite İçin Deney Tasarımı. *Electron. J. Mach. Technol.* **2009**, *6* (1), 71–83.

(52) Asiltürk, I.; Neşeli, S. Multi Response Optimisation of CNC Turning Parameters via Taguchi Method-Based Response Surface Analysis. *Meas. J. Int. Meas. Confed.* **2012**, *45* (4), 785–794. https://doi.org/10.1016/j.measurement.2011.12.004.

(53) Chen, Y. H.; Tam, S. C.; Chen, W. L.; Zheng, H. Y. Application of the Taguchi Method in the Optimization of Laser Micro-Engraving of Photomasks. *Int. J. Mater. Prod. Technol.* **1996**, *11* (3–4), 333–344. https://doi.org/10.1504/IJMPT.1996.036336.

(54) Karaağaoğlu, E. An Experimental Design Technique: Randomized Block Design. *Turkish J. Biochem.* **2013**, *38* (1), 1–4. https://doi.org/10.5505/tjb.2013.04796.

(55) Tekindal, M. A.; Bayrak, H.; Ozkaya, B.; Genc, Y. Box- Behnken Experimental Design in Factorial Experiments: The Importance of Bread for Nutrition and Health. *Turkish J. F. Crop.* **2012**, *17* (2), 115–123.

(56) Agarwal, A.; Kharb, V.; Saharan, V. A. Process Optimisation, Characterisation and Evaluation of Resveratrol-Phospholipid Complexes Using Box-Behnken Statistical Design. *Int. Curr. Pharm. J.* **2014**, *3* (7), 301–308. https://doi.org/10.3329/icpj.v3i7.19079.

(57) Taylan, D.; Özdemir, G. An Application of Taguchi's Design of Experiment, 2009, Vol. Yüksek Lis.

(58) Sahiner, S. The Basic Principles of Fitting Linear Regression Model By Least Squares. *MKÜ Ziraat Fakültesi Derg. 5* **2000**, *5* (1–2), 57–73.

(59) Anthony, D. Regression Analysis. *Nurse Res.* **1996**, *4* (1), 318–326. https://doi.org/10.7748/nr1996.10.4.1.318.c6066.

(60) Ross, S. M. Linear Regression. In *Introductory Statistics*; Elsevier, 2010; pp 537–604. https://doi.org/10.1016/B978-0-12-374388-6.00012-0.

(61) Loftus, S. C. Simple Linear Regression. In *Basic Statistics with R*; Elsevier, 2022; pp 227–247. https://doi.org/10.1016/B978-0-12-820788-8.00032-8.

(62) Ross, S. M. Linear Regression. In *Introductory Statistics*; Elsevier, 2017; pp 519–584. https://doi.org/10.1016/B978-0-12-804317-2.00012-6.

(63) Dover, J. L. *Probability and Statistics for Engineering and the Sciences*; 2005.

(64) Yalçın, F. B. An Application of Least Squares Method in Nonlinear Models-Solid Waste Sample. *Turkish J. Sci.* **2021**, *6* (2), 71–75.

(65) Pinder, J. P. Regression. In *Introduction to Business Analytics using Simulation*; Elsevier, 2017; pp 313–369. https://doi.org/10.1016/B978-0-12-810484-2.00010-4.

(66) Tian, M.; Su, Y. Multiple Nonlinear Regression Model for Predicting the Optical Performances of Dielectric Crossed Compound Parabolic Concentrator (DCCPC). *Sol. Energy* **2018**, *159*, 212–225. https://doi.org/10.1016/j.solener.2017.10.090.

(67) Hahn, G. J. The Coefficient of Determination Exposed. *Chem. Technol.* **1973**, *3* (10), 609–612.

(68) *Minitab*. https://blog.minitab.com/en/adventures-in-statistics-2/multiple-regession-analysis-use-adjusted-r-squared-and-predicted-r-squared-to-include-the-correct-number-of-variables.

(69) Miles, J. R Squared, Adjusted R Squared. In *Wiley StatsRef: Statistics Reference Online*; Wiley, 2014; pp 2–4. https://doi.org/10.1002/9781118445112.stat06627.

(70) Erten, H. İ. Optimum Design and Analysis of Torsion Spring Used in Series Elastic Actuators for Rehabilitation Robots, 2021.

(71) Jerez, T.; Kristjanpoller, W. Effects of the Validation Set on Stock Returns Forecasting. **2020**, *150*. https://doi.org/10.1016/j.eswa.2020.113271.

(72) Rao, S. S. *Engineering Optimization - Theory and Practice-Wiley (2009)*; 2009. https://doi.org/10.1002/9781119454816.

(73) Varaiya, P. *Stochastic Learning and Optimization: A Sensitivity-Based Approach*; 2008; Vol. 28. https://doi.org/10.1109/MCS.2008.929812.

(74) Punia, P.; Kaur, M. Various Genetic Approaches for Solving Single and Multi-Objective Optimization Problems: A Review. *Int. J. Adv. Res. Comput. Sci. Softw. Eng.* **2013**, *3* (7), 2277.

(75) Chang, K.-H. Multiobjective Optimization and Advanced Topics. In *e-Design*; Elsevier, 2015; pp 1105–1173. https://doi.org/10.1016/B978-0-12-382038-9.00019-3.

(76) Kumar, R.; Jagtap, H. P.; Rajak, D. K.; Bewoor, A. K. Traditional and Non-Traditional Optimization Techniques to Enhance Reliability in Process Industries; 2020; pp 67–80. https://doi.org/10.4018/978-1-7998-1464-1.ch004.

(77) Sreenivas, P.; Kumar, S. V. A Review on Non - Traditional Optimization Algorithm for Simultaneous Scheduling Problems. *IOSR J. Mech. Civ. Eng.* **2015**, *12* (2), 50–53. https://doi.org/10.9790/1684-12225053.

(78) ASM International. *ASM Handbook Volume 3: Alloy Phase Diagrams*; 1998.

(79) Roberts, G.; Krauss, G.; Kennedy, R. *Tool Steels*; Mesquita, R. A., Ed.; CRC Press, 2016. https://doi.org/10.1201/9781315181516.

(80) Mesquita, R. A. *Tool Steels Properties and Performance*; 2017.

(81) Aktekin, M. Investigation of The Welding Capability of Cold Work Tool Steel (DIN 1.2379) With Low Alloy Steels, 2022.

(82) Sohar, C. R. Lifetime Controlling Defects in Tool Steels. In *Springer Theses*; Springer Berlin Heidelberg: Berlin, Heidelberg, 2011; pp 215–224. https://doi.org/10.1007/978-3-642-21646-6_4.

(83) Abdul Rahim, M. A. S. Bin; Minhat, M. Bin; Hussein, N. I. S. B.; Salleh, M. S. Bin. A Comprehensive Review on Cold Work of AISI D2 Tool Steel. *Metall. Res. Technol.* **2018**, *115* (1), 104. https://doi.org/10.1051/metal/2017048.

(84) Conci, M. D.; Bozzi, A. Ô. C.; Franco, A. R. Effect of Plasma Nitriding Potential on Tribological Behaviour of AISI D2 Cold-Worked Tool Steel. *Wear* **2014**, *317* (1–2), 188–193. https://doi.org/10.1016/j.wear.2014.05.012.

(85) Costa, M. I.; Verdera, D.; Vieira, M. T. F.; Rodrigues, D. M. Surface Enhancement of Cold Work Tool Steels by Friction Stir Processing with a Pinless Tool. *Appl. Surf. Sci.* **2014**, *296*, 214–220. https://doi.org/10.1016/j.apsusc.2014.01.094.

(86) Salunkhe, S.; Fabijanic, D.; Nayak, J.; Hodgson, P. Effect of Single and Double Austenitization Treatments on the Microstructure and Hardness of AISI D2 Tool Steel. *Mater. Today Proc.* **2015**, *2* (4–5), 1901–1906. https://doi.org/10.1016/j.matpr.2015.07.145.

(87) Srithar, A.; Palanikumar, K.; Durgaprasad, B. Experimental Investigation and Surface Roughness Analysis on Hard Turning of AISI D2 Steel Using Coated Carbide Insert Experimental Investigation and Surface Roughness Analysis on Hard Turning of AISI D2 Steel Using Coated Carbide Insert. *Procedia Eng.* **2015**, *97* (January), 72–77. https://doi.org/10.1016/j.proeng.2014.12.226.

(88) Temmler, A.; Comiotto, M.; Ross, I.; Kuepper, M.; Liu, D. M.; Poprawe, R. Surface Structuring by Laser Remelting of 1.2379 (D2) for Cold Forging Tools in Automotive Applications. *J. Laser Appl.* **2019**, *31* (2), 022017. https://doi.org/10.2351/1.5070077.

(89) Moore, P.; Booth, G. Mechanical Testing of Welds. In *The Welding Engineers Guide to Fracture and Fatigue*; Elsevier, 2015; pp 113–141. https://doi.org/10.1533/9781782423911.2.113.

(90) Gong, Y.; Xu, J.; Buchanan, R. C. Surface Roughness: A Review of Its Measurement at Micro-/Nano-Scale. *Phys. Sci. Rev.* **2018**, *3* (1), 1–10. https://doi.org/10.1515/psr-2017-0057.

(91) Fiber Technology. 1µm Pulsed Fiber Laser ML20-PL-R-OEM. https://www.gmp.ch/htmlarea/pdf/Manlight/GMP_ML20-PL-R-OEM.pdf (accessed 2022-02-11).

APPENDIX A

DATA GROUPS

Table A.1. Training data (80%)

	Factor 1	**Factor 2**	**Factor3**	**Factor4**	**Output 1**	**Output 2**
Experimental Run	A:Average power	B:Repetition rate	C:Scan speed	D:Line spacing	Hardness	Roughness
	[W]	[kHz]	[mm/s]	[µm]	[HV0.5]	[µm]
1	10	20	10	20	342.00	0.77
2	10	20	10	30	304.67	0.57
4	10	20	50	20	312.67	0.38
5	10	20	50	30	350.00	0.50
6	10	20	50	40	317.33	0.39
7	10	20	90	20	336.67	0.36
8	10	20	90	30	303.33	0.48
9	10	20	90	40	306.00	0.42
11	10	60	10	30	340.67	0.53
12	10	60	10	40	318.33	0.63
13	10	60	50	20	299.67	0.33
14	10	60	50	30	289.67	0.49
15	10	60	50	40	313.00	0.40
16	10	60	90	20	378.33	0.35
18	10	60	90	40	317.67	0.32
19	10	100	10	20	374.67	0.62
20	10	100	10	30	330.67	0.67
22	10	100	50	20	335.67	0.51
23	10	100	50	30	319.67	0.47
25	10	100	90	20	304.67	0.60
26	10	100	90	30	356.67	0.37

(cont. on next page)

Table A.1 (cont.)

27	10	100	90	40	351.00	0.50
29	15	20	10	30	451.67	0.98
30	15	20	10	40	417.33	0.91
31	15	20	50	20	303.33	0.75
32	15	20	50	30	403.67	0.39
34	15	20	90	20	354.67	0.36
35	15	20	90	30	390.33	0.34
36	15	20	90	40	397.33	0.40
38	15	60	10	30	424.00	0.66
39	15	60	10	40	444.33	0.59
40	15	60	50	20	365.67	0.41
41	15	60	50	30	404.00	0.40
42	15	60	50	40	399.00	0.48
43	15	60	90	20	341.33	0.44
45	15	60	90	40	371.67	0.41
46	15	100	10	20	447.00	0.86
48	15	100	10	40	484.00	1.16
49	15	100	50	20	427.67	0.46
50	15	100	50	30	396.33	0.41
51	15	100	50	40	428.67	0.42
53	15	100	90	30	428.67	0.58
54	15	100	90	40	433.67	0.47
55	20	20	10	20	525.00	1.06
56	20	20	10	30	491.67	0.90
57	20	20	10	40	550.33	0.68
58	20	20	50	20	392.33	0.66
60	20	20	50	40	400.00	0.66
61	20	20	90	20	360.33	0.61
62	20	20	90	30	379.00	0.53

(cont. on next page)

Table A.1 (cont.)

63	20	20	90	40	409.67	0.77
64	20	60	10	20	482.00	0.65
65	20	60	10	30	448.00	0.82
67	20	60	50	20	411.67	0.68
68	20	60	50	30	398.67	0.52
69	20	60	50	40	393.00	0.68
70	20	60	90	20	389.00	0.65
71	20	60	90	30	367.00	0.60
73	20	100	10	20	401.00	1.12
74	20	100	10	30	498.33	1.28
75	20	100	10	40	468.00	1.37
76	20	100	50	20	445.00	0.51
78	20	100	50	40	401.67	0.62
79	20	100	90	20	358.00	0.63
80	20	100	90	30	353.00	0.57

Table A.2. Testing data 20%

	Factor 1	**Factor 2**	**Factor3**	**Factor4**	**Output 1**	**Output 2**
Experimental Run	A:Average power	B:Repetition rate	C:Scan speed	D:Line spacing	Hardness	Roughness
	[W]	[kHz]	[mm/s]	[µm]	[HV0.5]	[µm]
3	10	20	10	40	304.00	0.63
10	10	60	10	20	302.67	0.61
17	10	60	90	30	343.00	0.36
21	10	100	10	40	377.67	0.65
24	10	100	50	40	315.33	0.53
28	15	20	10	20	421.67	1.67
33	15	20	50	40	355.67	0.49
37	15	60	10	20	429.67	0.80
44	15	60	90	30	384.67	0.35
47	15	100	10	30	389.00	0.99
52	15	100	90	20	397.67	0.54
59	20	20	50	30	377.00	0.71
66	20	60	10	40	492.67	0.86
72	20	60	90	40	382.33	0.67
77	20	100	50	30	395.33	0.57
81	20	100	90	40	357.00	0.65

Table A.3. Validation data 10%

	Factor 1	**Factor 2**	**Factor3**	**Factor4**	**Output 1**	**Output 2**
Experimental Run	A:Average power	B:Repetition rate	C:Scan speed	D:Line spacing	Hardness	Roughness
	[W]	[kHz]	[mm/s]	[µm]	[HV0.5]	[µm]
9	10	20	90	40	306.00	0.42
18	10	60	90	40	317.67	0.32
26	10	100	90	30	356.67	0.37
32	15	20	50	30	403.67	0.39
39	15	60	10	40	444.33	0.59
51	15	100	50	40	428.67	0.42
56	20	20	10	30	491.67	0.90
64	20	60	10	20	482.00	0.65
75	20	100	10	40	468.00	1.37

APPENDIX B

REGRESSION CODE FOR HARDNESS (SECOND ORDER MULTIPLE NON-LINEAR (SON))

```
Clear["Global`*"]
 (* TRAINING DATA
A80={10,10,10,10,10,10,10,10,10,10,10,10,10,10,10,10,10,10,10,10,10,15,15,15,15,15,
15,15,15,15,15,15,15,15,15,15,15,15,15,15,15,15,20,20,20,20,20,20,20,20,20,20,20,
20,20,20,20,20,20,20,20,20,20,20};
B80={20,20,20,20,20,20,20,60,60,60,60,60,60,60,100,100,100,100,100,100,100,20,20,
20,20,20,20,20,20,60,60,60,60,60,60,60,100,100,100,100,100,100,100,100,20,20,20,20,20
,20,20,60,60,60,60,60,60,60,60,100,100,100,100,100,100,100};
C80={10,10,10,50,50,90,90,10,10,10,50,50,90,90,10,10,10,50,50,90,90,10,10,10,50,50,
90,90,10,10,50,50,90,90,90,10,10,50,50,50,90,90,90,10,10,50,50,50,90,90,10,10,10,50,
50,50,90,90,10,10,50,50,50,90,90};
D80={20,30,40,30,40,20,30,20,30,40,20,40,20,30,20,30,40,30,40,20,40,20,30,40,30,40,
20,30,20,40,20,30,20,30,40,20,30,20,30,40,20,30,40,30,40,20,30,40,20,40,20,30,40,20,
30,40,30,40,20,40,20,30,40,30,40};
H80={342.00,304.67,304.00,350.00,317.33,336.67,303.33,302.67,340.67,318.33,299.6
7,313.00,378.33,343.00,374.67,330.67,377.67,319.67,315.33,304.67,351.00,421.67,45
1.67,417.33,403.67,355.67,354.67,390.33,429.67,444.33,365.67,404.00,341.33,384.67,
371.67,447.00,389.00,427.67,396.33,428.67,397.67,428.67,433.67,491.67,550.33,392.
33,377.00,400.00,360.33,409.67,482.00,448.00,492.67,411.67,398.67,393.00,367.00,3
82.33,401.00,468.00,445.00,395.33,401.67,353.00,357.00};
 data1=Table[{A80[[i]],B80[[i]],C80[[i]],D80[[i]],H80[[i]]},{i,1,Length[H80]}];
 modelnn=Expand[(1+x1+x2+x3+x4)^2];
CC=Table[a[i],{i,1,Length[modelnn]}];
DD=Table[b[i],{i,1,Length[modelnn]}];
AA=Table[(CC[[i]]modelnn[[i]]),{i,1,Length[modelnn]}]//Total;
BB=Table[(DD[[i]]modelnn[[i]]),{i,1,Length[modelnn]}]//Total;
coef={CC,DD}//Flatten;
TT=AA/BB;
 constIE=NonlinearModelFit[data1,AA,coef,{x1,x2,x3,x4}]
 FittedModel[ -48.4232 + <<17>> + 0.00159865 x3 x4 + 0.0205614 x4^2 ]
 modelIE=constIE//Normal
 -48.4232+53.7464 x1-1.28954 x1^2+0.289413 x2-0.0510991 x1 x2+0.00347891
x2^2+0.235088 x3-0.137998 x1 x3+0.00320769 x2 x3+0.00990613 x3^2-2.58042
x4+0.113778 x1 x4-0.0000332097 x2 x4+0.00159865 x3 x4+0.0205614 x4^2
 -48.423171404381456`+53.746398210513966` x1-1.2895367785586829`
x1^2+0.2894129750949088` x2-0.05109906686120986` x1 x2+0.003478914190986649`
x2^2+0.23508834667309295` x3-0.13799804738829238` x1
x3+0.0032076905247195977` x2 x3+0.009906130971054996` x3^2-
```

2.5804182412177843` x4+0.11377801148037163` x1 x4-0.00003320972605374342` x2 x4+0.0015986507618359755` x3 x4+0.020561419127851806` $x4^2$

-48.4232+53.7464 x1-1.28954 $x1^2$+0.289413 x2-0.0510991 x1 x2+0.00347891 $x2^2$+0.235088 x3-0.137998 x1 x3+0.00320769 x2 x3+0.00990613 $x3^2$-2.58042 x4+0.113778 x1 x4-0.0000332097 x2 x4+0.00159865 x3 x4+0.0205614 $x4^2$

(modelIE)/.x1->A/.x2->B/.x3->C/.x4->D

-48.4232+53.7464 A-1.28954 A^2+0.289413 B-0.0510991 A B+0.00347891 B^2+0.235088 C-0.137998 A C+0.00320769 B C+0.00990613 C^2-2.58042 D+0.113778 A D-0.0000332097 B D+0.00159865 C D+0.0205614 D^2

R2training=constIE[{"RSquared","AdjustedRSquared"}]

{0.996052,0.992668}

constIE[{"PredictedResponse","Response"}]//Transpose//TableForm

{
{326.909, 342.},
{322.916, 304.67},
{323.036, 304.},
{305.38, 350.},
{306.139, 317.33},
{322.256, 336.67},
{319.543, 303.33},
{330.435, 302.67},
{326.429, 340.67},
{326.535, 318.33},
{317.391, 299.67},
{314.771, 313.},
{336.047, 378.33},
{333.32, 343.},
{345.093, 374.67},
{341.074, 330.67},
{341.167, 377.67},
{333.802, 319.67},
{334.535, 315.33},
{360.97, 304.67},
{359.602, 351.},
{433.817, 421.67},
{435.513, 451.67},
{441.322, 417.33},
{390.377, 403.67},
{396.825, 355.67},
{373.965, 354.67},
{376.94, 390.33},
{427.123, 429.67},
{434.601, 444.33},
{386.479, 365.67},
{388.802, 404.},
{377.536, 341.33},
{380.498, 384.67},

```
 {387.572, 371.67},
 {431.561, 447.},
 {433.231, 389.},
 {396.05, 427.67},
 {398.36, 396.33},
 {404.781, 428.67},
 {392.239, 397.67},
 {395.188, 428.67},
 {402.249, 433.67},
 {483.633, 491.67},
 {495.131, 550.33},
 {402.872, 392.33},
 {410.897, 377.},
 {423.034, 400.},
 {361.197, 360.33},
 {382.638, 409.67},
 {459.334, 482.},
 {466.706, 448.},
 {478.19, 492.67},
 {391.091, 411.67},
 {399.103, 398.67},
 {411.226, 393.},
 {363.199, 367.},
 {375.962, 382.33},
 {453.553, 401.},
 {472.383, 468.},
 {390.442, 445.},
 {398.44, 395.33},
 {410.551, 401.67},
 {367.669, 353.},
 {380.419, 357.}
}
 (* TESTING DATA
 A20={10,10,10,10,10,10,15,15,15,15,15,20,20,20,20,20};
B20={20,20,60,60,100,100,20,20,60,60,100,20,20,60,100,100};
C20={50,90,50,90,50,90,50,90,10,50,10,10,90,90,10,90};
D20={20,40,30,40,20,30,20,40,30,40,40,20,30,20,30,20};
H20={312.67,306.00,289.67,317.67,335.67,356.67,303.33,397.33,424.00,399.00,484.0
0,525.00,379.00,389.00,498.33,358.00};
datatest=Table[{A20[[i]],B20[[i]],C20[[i]],D20[[i]],H20[[i]]},{i,1,Length[H20]}]//TableFor
m;
 H20predicted=Table[modelIE/.x1->A20[[i]]/.x2->B20[[i]]/.x3->C20[[i]]/.x4-
>D20[[i]],{i,1,Length[H20]}]
{308.733,320.942,314.025,334.706,337.182,358.23,388.041,384.028,428.806,395.237,
439.013,476.248,369.861,354.548,460.911,359.031}
 Table[{H20[[i]],H20predicted[[i]]},{i,1,Length[H20]}]//TableForm
 { {312.67, 308.733},
```

{306., 320.942},
{289.67, 314.025},
{317.67, 334.706},
{335.67, 337.182},
{356.67, 358.23},
{303.33, 388.041},
{397.33, 384.028},
{424., 428.806},
{399., 395.237},
{484., 439.013},
{525., 476.248},
{379., 369.861},
{389., 354.548},
{498.33, 460.911},
{358., 359.031}}

$$\text{SSE}=\sum_{i=1}^{\text{Length[B20]}} (\text{H20[[i]]}-\text{H20predicted[[i]]})^2$$

15589.3

Hbar=Mean[H20]

379.709

$$\text{SST}=\sum_{i=1}^{\text{Length[B20]}} (\text{H20[[i]]}-\text{Hbar})^2$$

79446.6

R2testing=1-SSE/SST

0.803777

(*Validation Data

A10={10,10,10,15,15,15,20,20,20};

B10={20,60,100,20,60,100,20,60,100};

C10={10,50,90,50,10,50,90,50,10};

D10={30,20,40,30,40,20,40,30,20};

H10={304.67,299.67,351.00,403.67,444.33,427.67,409.67,398.67,401.00};

datavalidation=Table[{A10[[i]],B10[[i]],C10[[i]],D10[[i]],H10[[i]]},{i,1,Length[H10]}]//TableForm;

Length[H10]

9

H10predicted=Table[modelIE/.x1->A10[[i]]/.x2->B10[[i]]/.x3->C10[[i]]/.x4->D10[[i]],{i,1,Length[H10]}]

{322.916,317.391,359.602,390.377,434.601,396.05,382.638,399.103,453.553}

Table[{H10[[i]],H10predicted[[i]]},{i,1,Length[H10]}]//TableForm

{

{304.67, 322.916},
{299.67, 317.391},
{351., 359.602},
{403.67, 390.377},
{444.33, 434.601},
{427.67, 396.05},
{409.67, 382.638},

{398.67, 399.103},
{401., 453.553}
}

$$SSE2=\sum_{i=1}^{Length[B10]}(H10[[i]]-H10predicted[[i]])^2$$

5484.82

H10bar=Mean[H10]

382.261

$$SST2=\sum_{i=1}^{Length[B10]}(H10[[i]]-H10bar)^2$$

21563.4

R2validation=1-SSE2/SST2

0.745642

Max[A80]

20

Max[B80]

100

Max[C80]

90

Max[D80]

40

Min[A80]

10

Min[B80]

20

Min[C80]

10

Min[D80]

20

maxvalue=NMaximize[{modelIE,Min[A80]<=x1<=Max[A80],Min[B80]<=x2<=Max[B80],
Min[C80]<=x3<=Max[C80],Min[D80]<=x4<=Max[D80]},{x1,x2,x3,x4}]

{495.131,{x1->20.,x2->20.,x3->10.,x4->40.}}

maxvalue[[1]]

495.131

minvalue=NMinimize[{modelIE,Min[A80]<=x1<=Max[A80],Min[B80]<=x2<=Max[B80],
Min[C80]<=x3<=Max[C80],Min[D80]<=x4<=Max[D80]},{x1,x2,x3,x4}]

{305.14,{x1->10.,x2->20.,x3->51.8797,x4->33.0805}}

minvalue[[1]]

305.14

(* R2 training, R2 training adjusted, R2 testing, R2 validation, Max, Min
Results={R2training[[1]],R2training[[2]],R2testing,R2validation,maxvalue[[1]],minvalue[
[1]]}

{0.996052,0.992668,0.803777,0.745642,495.131,305.14}

APPENDIX C

OPTIMIZATION CODE FOR HARDNESS

```
Clear["Global'*"]
 modelroughness=(13.101401369628958` -0.6017149469534143`
Log[x1]+0.224076548965367` Log[x1]^2-2.197884204350617` Log[x2]-
0.026019674360441367` Log[x1] Log[x2]+0.2034392270308284` Log[x2]^2-
0.9750349690897032` Log[x3]-0.12038213038747095` Log[x1]
Log[x3]+0.026352255795680922` Log[x2] Log[x3]+0.09202525848454077` Log[x3]^2-
3.6569776646819023` Log[x4]+0.08270606484083204` Log[x1]
Log[x4]+0.18517796804950598` Log[x2] Log[x4]+0.12217230592057576` Log[x3]
Log[x4]+0.33601719919784856` Log[x4]^2)/.x1->A/.x2->B/.x3->C/.x4->D
 13.1014 -0.601715 Log[A]+0.224077 Log[A]^2-2.19788 Log[B]-0.0260197 Log[A]
Log[B]+0.203439 Log[B]^2-0.975035 Log[C]-0.120382 Log[A] Log[C]+0.0263523 Log[B]
Log[C]+0.0920253 Log[C]^2-3.65698 Log[D]+0.0827061 Log[A] Log[D]+0.185178 Log[B]
Log[D]+0.122172 Log[C] Log[D]+0.336017 Log[D]^2
modelIE=(-48.423171404381456`+53.746398210513966` x1-1.2895367785586829`
x1^2+0.2894129750949088` x2-0.05109906686120986` x1 x2+0.003478914190986649`
x2^2+0.23508834667309295` x3-0.13799804738829238` x1
x3+0.0032076905247195977` x2 x3+0.009906130971054996` x3^2-
2.5804182412177843` x4+0.11377801148037163` x1 x4-0.00003320972605374342`
x2 x4+0.0015986507618359755` x3 x4+0.020561419127851806` x4^2)
 -48.4232+53.7464 x1-1.28954 x1^2+0.289413 x2-0.0510991 x1 x2+0.00347891
x2^2+0.235088 x3-0.137998 x1 x3+0.00320769 x2 x3+0.00990613 x3^2-2.58042
x4+0.113778 x1 x4-0.0000332097 x2 x4+0.00159865 x3 x4+0.0205614 x4^2
 modelhardness=(modelIE)/.x1->A/.x2->B/.x3->C/.x4->D
 -48.4232+53.7464 A-1.28954 A^2+0.289413 B-0.0510991 A B+0.00347891 B^2+0.235088
C-0.137998 A C+0.00320769 B C+0.00990613 C^2-2.58042 D+0.113778 A D-
0.0000332097 B D+0.00159865 C D+0.0205614 D^2

a1=NMinimize[{modelhardness,10<=A<=20,20<=B<=100,10<=C<=90,20<=D<=40},{A,B,
C,D},Method->"NelderMead"]
 {305.14,{A->10.,B->20.,C->51.8797,D->33.0805}}

a2=NMaximize[{modelhardness,10<=A<=20,20<=B<=100,10<=C<=90,20<=D<=40},{A,B,
C,D},Method->"NelderMead"]
 {495.131,{A->20.,B->20.,C->10.,D->40.}}
 minroughhness=modelroughness/.{A->10.`,B->20.`,C->51.87969570779657`,D-
>33.08051835841795`}
 0.381348
 maxroughhness=modelroughness/.{A->20.`,B->20.`,C->10.`,D->40.`}
 0.99234

a12=NMinimize[{modelhardness,10<=A<=20,20<=B<=100,10<=C<=90,20<=D<=40},{A,B
```

```
,C,D},Method->"DifferentialEvolution"]
 {305.14,{A->10.,B->20.,C->51.8794,D->33.0805}}

a22=NMaximize[{modelhardness,10<=A<=20,20<=B<=100,10<=C<=90,20<=D<=40},{A,
B,C,D},Method->"DifferentialEvolution"]
 {495.131,{A->20.,B->20.,C->10.,D->40.}}

a13=NMinimize[{modelhardness,10<=A<=20,20<=B<=100,10<=C<=90,20<=D<=40},{A,B
,C,D},Method->"SimulatedAnnealing"]
 {305.14,{A->10.,B->20.,C->51.8797,D->33.0805}}

a23=NMaximize[{modelhardness,10<=A<=20,20<=B<=100,10<=C<=90,20<=D<=40},{A,
B,C,D},Method->"SimulatedAnnealing"]
 {495.131,{A->20.,B->20.,C->10.,D->40.}}

a14=NMinimize[{modelhardness,10<=A<=20,20<=B<=100,10<=C<=90,20<=D<=40},{A,B
,C,D},Method->"RandomSearch"]
 {305.14,{A->10.,B->20.,C->51.8797,D->33.0805}}

a24=NMaximize[{modelhardness,10<=A<=20,20<=B<=100,10<=C<=90,20<=D<=40},{A,
B,C,D},Method->"RandomSearch"]
{495.131,{A->20.,B->20.,C->10.,D->40.}}
```